Strong Ionizing Shock Waves

ROBERT A. GROSS
Columbia University, New York, New York

The physical effects created by strong shock waves propagating in hydrogen are reviewed and theoretically studied for speeds up to relativistic conditions. In the progression from weak to relativistic shock speeds, various physical phenomena affect the shock wave. Dissociation, ionization, and the presence of an upstream electric field cause several important effects for slow (sub-Alfvénic speed) normal ionizing shock waves. Switch-on shock behavior is extended to slow ionizing waves. The effect of radiation is investigated for both the optically thick and thin cases. Relativistic shock jump equations are solved for wave speeds approaching the speed of light. Thermonuclear shock solutions are examined. The theory of the electromagnetically driven shock tube is reviewed and the corresponding shock tube problem is explored. Wave stability is reviewed. Experimental results on strong ionizing shock waves are reviewed and discussed.

I. INTRODUCTION

All of physics is involved in understanding completely all shock wave phenomena. Alternatively, shock waves are being used in the laboratory to study physics. Shock waves can create states of matter which are difficult or impossible to produce in any other way; e.g., a thermalized plasma at very high temperature and pressure. Yet the range of shock conditions that have been explored in depth, either analytically or experimentally, has been relatively small. This paper reviews the status and some of the recent results of research on very high speed shock waves. Particular attention is given to ionizing shock waves where the pre-shock state of the gas is nonconducting and the post-shock state is ionized and a good electrical conductor. Behavior of an electromagnetically driven shock wave propagating through hydrogen is theoretically studied at speeds up to and including relativistic conditions. In the progression from weak to relativistic shock speeds various physical phenomena affect the shock wave. Attention is centered upon these physical effects in this paper.

Consider diatomic hydrogen at 273°K, a pressure of 0.10 Torr, and in the presence of a magnetic field of 1.38 Wb/m². The direction of the magnetic field is normal to the plane of the shock wave and such waves are called normal shock waves. This physical state of hydrogen is typical of conditions in which laboratory shock waves are created. In the remainder of this paper this initial state of hydrogen will, in most cases, be taken as the typical example.

An ionizing shock is defined as a compressive wave which propagates into a nonionized, nonconducting gas, ionizes it, and thus makes the post-shock gas electrically conducting and capable of interacting with an electromagnetic field. In Fig. 1 is shown the temperature of the shock-heated gas that is produced by a shock wave in hydrogen (at the above initial state conditions) as the speed of propagation increases from a sound wave (sonic speed, $a_1 = 1.25\times10^3$ m/sec) to relativistic speeds (speed of light, $c=3\times10^8$ m/sec). Various branches of this curve correspond to the emergence of physical phenomena which are characteristic of the speed regime of the shock wave. Figure 2 shows the density ratio (the final to initial state) of the gas throughout this same speed range.

At low shock wave speeds, namely, $u_1 \leq 6\times10^3$ m/sec which corresponds to a shock Mach number $M_1 = u_1/a_1 \leq 5$ the shock jump conditions are determined from the well-known Rankine–Hugoniot equations for a nonconducting gas. Dissociation of the shocked gas occurs for wave speeds where

$$6\times10^3 < u_1 < 2.5\times10^4 \text{ m/sec.}$$

The latter speed corresponds to Mach 20 and the post-shock gas consists mainly of monatomic hydrogen. Ionization of the hydrogen atom takes place for wave speeds in the range

$$2.5\times10^4 \text{ m/sec} < u_1 < 7\times10^4 \text{ m/sec.}$$

The shocked gas produced by a wave whose speed is 7×10^4 m/sec (Mach 56, 25 000°K) is essentially a completely ionized hydrogen plasma consisting of electrons and protons. The chemical composition of the equilibrium post-shock state is shown in Fig. 3. Below a shock speed of about 1×10^4 m/sec the shock wave can be produced in a pressure-driven shock tube and the state of the shocked gas can be predicted well by conventional aerodynamic shock wave theory. Above about Mach 20 ($u_1 > 2.5\times10^4$ m/sec) ionization of hydrogen becomes significant, electromagnetic phenomena becomes important, and it is here that the study of an ionizing shock wave begins.

II. SLOW IONIZING SHOCK WAVES

A slow ionizing shock wave is defined as a compressive shock whose post-shock state is ionized and which propagates with sub-Alfvénic speed. The Alfvén speed b_x is defined by

$$b_x^2 = \mu H_x^2/\rho, \tag{1}$$

where H_x is the magnetic field normal to the shock, ρ the gas density, and μ is the magnetic permeability. In this review $a_1 < b_1$ always, unless otherwise noted. In the nonconducting pre-shock gas, Alfvén waves do not propagate but it is convenient to introduce this speed in describing various ionizing shock wave regimes. In Fig. 1, slow ionizing shock waves correspond to waves speeds $u_1 < 3.58 \times 10^5$ m/sec.

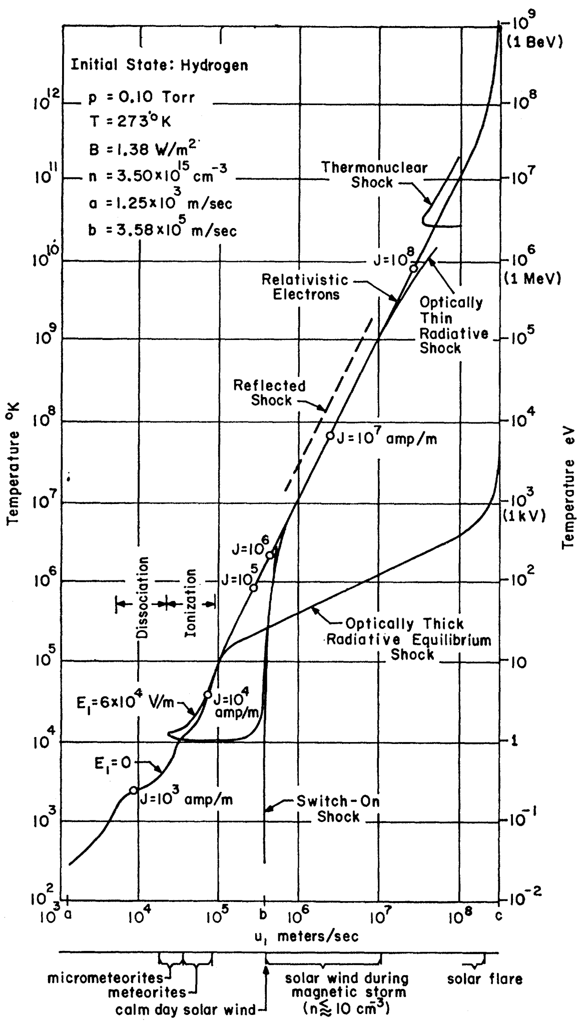

FIG. 1. Post-shock temperature vs wave speed.

Figure 4 displays the shock frame coordinates. The steady-jump equations across a normal ionizing shock

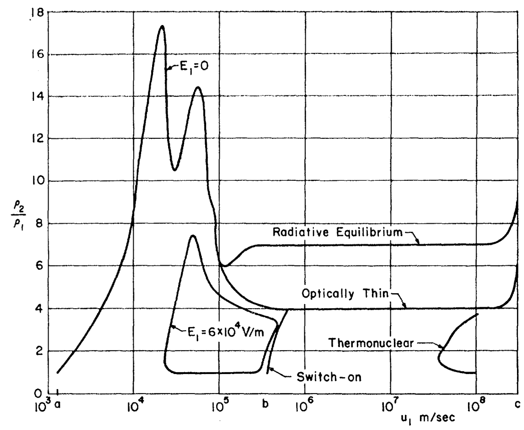

FIG. 2. Density ratio vs wave speed.

wave are

$$\rho_1 u_1 = \rho_2 u_2 = m, \tag{2}$$

$$m u_1 + p_1 = m u_2 + p_2 + \tfrac{1}{2}(\mu H_z^2), \tag{3}$$

$$m w_2 - \mu H_x H_{z2} = 0, \tag{4}$$

$$m(\tfrac{1}{2}u_1^2 + h_1) = m[\tfrac{1}{2}(u_2^2 + w_2^2) + h_2] + E_y H_{z2}, \tag{5}$$

where the u's are velocities relative to the shock front, and 1, 2 refer to pre- and post-shock states, respectively. The pre-shock gas is assumed at rest in the laboratory frame. The shock speed is then u_1, and the longitudinal magnetic field $H_x > 0$ is constant everywhere. These equations represent conservation of mass, momentum and energy, where ρ is the gas density, p the gas pressure, h the enthalpy, and the vector components of the velocity (u, w) and magnetic field (H_x, H_z) are illustrated in Fig. 4. The upstream neutral gas transverse electric field in the laboratory coordinate reference frame E_{L_1} is the same as that in the shock coordinate reference frame E_y, since the magnetic field is parallel to the shock velocity. Thus,

$$E_{L_1} = E_y + u_1 \times B_1 = E_y. \tag{6}$$

In region 2, for a steady state to exist, no current must flow and the usual MHD relation applies, namely,

$$E_y = -u_2 \times B_2. \tag{7}$$

Since the transverse electric field is constant in the

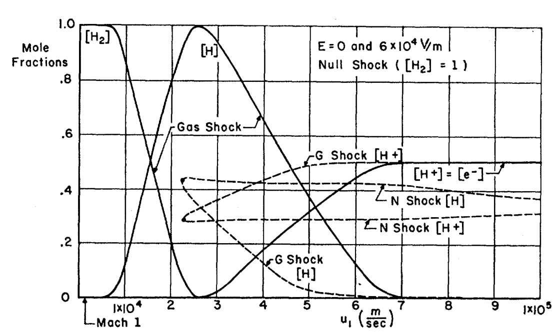

FIG. 3. Post-shock chemical composition for hydrogen.

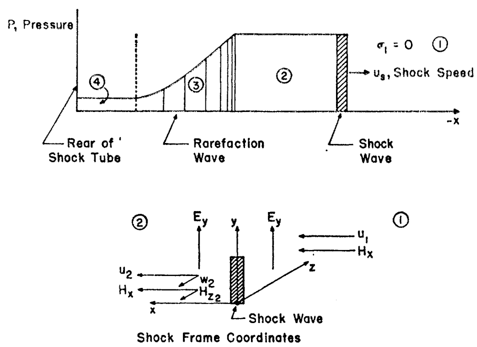

Fig. 4. Shock coordinate systems.

shock frame (but not in the lab frame) across the ionizing shock,

$$E_y = \mu(u_2 H_{z2} - w_2 H_z) = E_{L1}. \tag{8}$$

Across the ionizing shock wave there is a change in the chemical composition represented by the following reaction equation,

$$H_2 \cdot \rightarrow \alpha_1 H_2 + \alpha_2 H + \alpha_3 H^+ + \alpha_4 e^-, \tag{9}$$

where one mole of diatomic hydrogen in the pre-shock state is converted to α_1 moles of H_2, α_2 moles of monatomic hydrogen, etc, H^+ and e^- being protons and electrons. The assumption of chemical equilibrium in the post-shock state gives two further relations:

$$K_{H_2}(T_2) = x_1/x_2^2 p_2 \quad \text{for} \quad H_2 \rightleftarrows 2H \tag{10}$$

$$K_H(T_2) = x_2/x_3 x_4 p_2 \quad \text{for} \quad H \rightleftarrows H^+ + e^-, \tag{11}$$

where $K_i(T)$ are the equilibrium constants and x_i are the mole fractions defined by

$$x_i = \alpha_i / \sum \alpha_j. \tag{12}$$

In Eq. (5), the enthalpy h_2 for the post-shock state is that for a mixture of ideal gases, namely,

$$h_2 = \sum x_i h_i. \tag{13}$$

If all the pre-shock conditions, including the transverse electric field are specified, then the foregoing set of equations, together with the relevant thermochemical data, constitute a complete set of nonlinear algebraic equations which determine uniquely the post-shock states.

However, *for ionizing shock waves one cannot arbitrarily specify the pre-shock electric field* E_y. This is the first new feature which distinguishes ionizing shocks from MHD shocks (where $E_y = 0$) and gas dynamic shocks, where the electric field is irrelevant. Several authors (1–8) recognized this physical fact and the recent work of C. K. Chu (8) has clarified mathematically the correct approach for formulating properly posed initial-boundary value problems involving ionizing shock waves. In general, an electromagnetic wave propagates ahead of the shock thus eliminating the arbitrariness in the fields present at the initiation of the shock. The source of this electric field originates in the ionizing shock structure. An analytical prediction of E_y requires an accurate and physically correct solution of the ionizing wave structure. This is beyond present capability although a simple model developed by Kulikovskii (1) and Chu (8) illustrates the basic principles.

Regarding E_y as a parameter, the system of jump equations can be solved explicitly. This has been done in thorough detail by R. Taussig (9, 10). Experiments performed by B. Miller (11) at Columbia University have given a guide as to the order of magnitude of E_y, which for slow ionizing waves is of the order of a hundred volts per centimeter. The two curves in Fig. 1 corresponds to $E_1 = 0$ and $E_1 = 6 \times 10^2$ V/cm.

The ionizing shock wave jump solutions are contiguous with the low speed aerodynamic shock solution for the case of $E_1 = 0$. However, for $E_1 > 0$, the second new feature of ionizing waves occurs. *The ionizing shock wave solutions are bounded for a given* E_1 *and below a certain speed* (determined by the pre-shock conditions) *there are no steady-state solutions*. In Fig. 1 are shown numerical solutions of the conservation jump equations for $E_1 = 600$ V/cm. The minimum speed for a steady solution in this case is about 2.3×10^4 m/sec. This particular speed represents a singular point where the so-called (N) and (G) shock solutions merge. [So called because they lie adjacent to the null ($\rho_1 = \rho_2$ when $E_1 = 0$) and gas dynamic shock solutions, respectively.] It is similar to (but not identical to) a Chapman Jouguet point for exothermal waves (5). A third new feature of ionizing shock waves with an electric field is that *the post ionizing shock temperature is higher than that produced by the corresponding zero field shock wave moving at the same speed*. The electric field has added energy to the system.

A fourth new feature of ionizing waves is that *there is a value of the electric field* E^**, such that above this value of electric field there is no steady solution for slow ionizing waves*. This point has been examined by Taussig (9) who has shown that this critical value of the electric field is given by

$$E^* = 0.357[B_x^2/(\mu\rho_1)^{\frac{1}{2}}] \qquad u_1 < b_{x1} \quad \gamma = \tfrac{5}{3}. \tag{14}$$

However, since the initial electrical field cannot be prescribed, E^* probably represents an upper bound for the pre-shock electric field state. For fields larger than E^*, no steady compressive slow shock solutions exist, and this situation is unparalleled in either pure gas or hydromagnetic shocks.

The effect of a transverse electric field upon the density ratio of slow ionizing shock waves is quite significant as can be seen in Fig. 2. The greater the value of E_1, the larger the deviation from the usual gas dynamic case until $E_1 \geq E^*$ when steady ionizing waves are no longer possible.

The physical origin of the electric field E in the pre-shock nonconducting gas is worthy of discussion. First consider a shock tube which initially contains a cold, nonconducting gas at rest in the laboratory. An axial magnetic field H_x is externally applied. If a large voltage is applied radially across the shock tube (for example from an inner to outer co-axial cylinder), the gas will break down, radial current will flow, and the ionized gas conducting the radial current will begin to rotate as a result of the Lorentz force from the radial current and axial magnetic field. The electric charge initially distributed along the shock tube walls will flow through the ionized gas and redistribution of charge along the boundaries will alter the large initial electric field in the cold gas. A steady state will have developed when the charge distribution along the shock tube produces an upstream electric field E_1 (in the laboratory reference frame) in the pre-shocked gas. In the shock frame, the tangential electric field across the shock wave is conserved as required by Maxwell's equations. The basic source of this electric field in this physical situation may be viewed as resulting from the electrostatic charge redistribution on the tube walls during the gas breakdown and acceleration phase.

If there is no axial field but only a magnetic field parallel to the plane of the shock wave (transverse shock), then the ionized gas in and behind the shock wave will have, as a result of its motion, an induced electric field. Current will flow, and during the shock wave acceleration, charge along the boundaries will be redistributed so that the tangential electric field on both sides of the shock wave is constant. This transverse ionizing shock case will generate an upstream electric field even in the case of the ordinary pressure gas-driven shock tube. If the shock tube walls are a dielectric, they become polarized and the same qualitative effect should be found, but the exact physical situation and boundary conditions are more complex.

In summary, whenever electric currents flow parallel to the shock plane, either from the driving mechanism such as in the electromagnetic shock tube, or induced currents resulting from conducting gas moving across a magnetic field, a nonzero tangential electric field in the pre-shock gas is established which has important consequences on the jump properties of ionizing shock waves.

III. SWITCH-ON BEHAVIOR

Another feature of slow ionizing waves with a transverse electric field is that such waves exhibit "switch-on" behavior at sub-Alfvénic speeds. A switch-on shock in magnetohydrodynamics is one in which the transverse magnetic field and transverse component of momentum are nonzero behind the shock while these quantities were zero in the pre-shock state. The magnetic field and momentum are switched on by the shock wave. This switch-on state is caused by current flowing through the structure of the shock wave.

In conventional magnetohydrodynamics switch-on

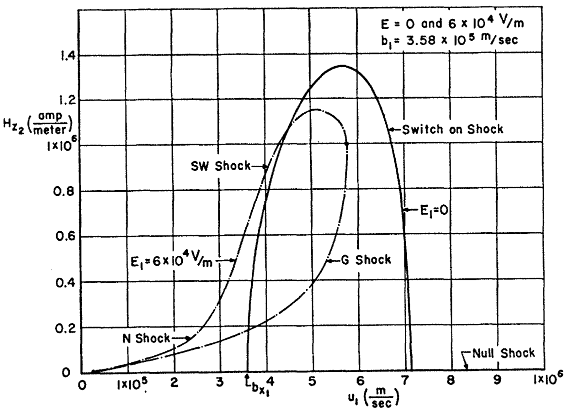

FIG. 5. Switch-on magnetic field.

shocks occur only for the following speed regime:

$$1 \leq \frac{u_1^2}{b_{x_1}^2} \leq \frac{(\gamma+1)\frac{1}{2}M_1^2}{1+(\gamma-1)\frac{1}{2}M_1^2} \approx 4 \quad (\text{for } \gamma=\tfrac{5}{3}) \qquad (15a)$$

and

$$a_1/b_1 < 1. \qquad (15b)$$

There are no switch-on shocks for $a_1/b_1 > 1$.

The usual switch-on solution can be seen in Figs. 1 and 2 as the branch beginning at $u_1 = b_1 = 3.58 \times 10^5$ m/sec and merging with the gas dynamic solution at a wave speed of about $2b_1$. The appearance and disappearance of the switch-on wave is a matter closely related to wave stability, which is discussed in a later section. In Fig. 5 are some results of the switch-on magnetic field at sub-Alfvénic speeds and they can be compared with the usual zero E field switch-on case. The effect of current flowing through the shock wave and the resultant magnetic field change can be tested in experiments. Miller (11) in experiments with electromagnetically driven slow ionizing waves, has measured this switch-on-like behavior at sub-Alfvénic speeds.

IV. SHOCK STRUCTURE

The problem of determining gas dynamic shock wave structure (i.e., the structure of the region which separates the shock equilibrium jump states) when the gas is considered to have finite transport properties (viscosity and thermal conductivity) and to behave according to the Navier–Stokes equations was first undertaken by Becker (12) and in its most general form by Gilbarg and Paolucci (13, 14). Other authors, notably Wang Chang (15), Mott Smith (16), Zoller (17), and Grad (18) have undertaken the solution of the problem by direct application of the Boltzmann equation.

The structure of an MHD shock is more complicated. In the general Navier–Stokes description, four simultaneous first-order nonlinear differential equations must be integrated between equilibrium points. For transverse shocks the number of equations is reduced

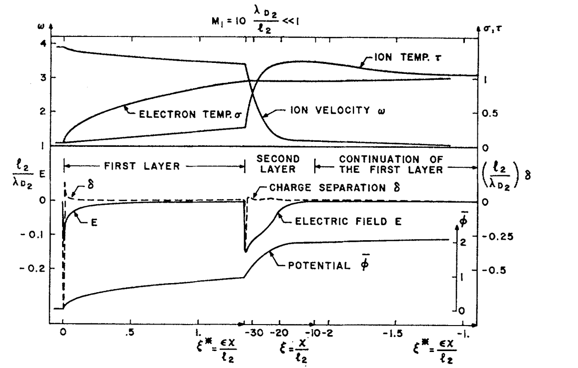

FIG. 6. Distribution of flow and electrical variables through a strong shock in a plasma.

to three. Magnetogasdynamic shock structure has been studied by Marshall (19), Burgers (20), Ludford (21), Germain (22), Tverskoi (23), Deutsch (24), Bleviss (134), and Anderson (25). In none of these works, however, is a numerical integration of more than two simultaneous equations attempted, the order of the problem being reduced by the assumption that certain of the transport coefficients are zero. The difficult problem of the integration of more than two simultaneous first-order differential equations is discussed theoretically by Anderson (25) and by Nemytskii and Stapanov (26).

The structure of a multifluid shock wave in a completely ionized gas in the absence of any externally applied magnetic or electric fields has been studied by Jaffrin and Probstein (27) and by Imshennik (28). Jaffrin and Probstein use the Navier–Stokes equations for electron and ion fluids, together with Poisson's equation for the self-induced electric field. When the Debye length downstream of the shock is small compared to the ion–ion mean free path there, the plasma remains essentially neutral and the equations governing the charge separation and electric field can be uncoupled from the system. When the Mach number is greater than 1.12 an ion shock appears imbedded in a wider electron thermal layer. When the shock is strong, a precursor electric shock layer appears upstream at the beginning of the thermal layer. Calculations at Mach 10 show that in the imbedding electric shock layer, there is a relative excess of electrons of approximately 50% locally and there are damped ion oscillations present. Figure 6 from Jaffrin and Probstein's work shows the distribution of flow and electrical variables through a strong shock ($M_1 = 10$) for the case of small Debye length. The abscissa of Fig. 6 refers to several dimensionless lengths where $\epsilon = (m_e/m_i)^{\frac{1}{2}}$ and l refers to the mean free path in the region indicated by the subscript. The ordinates refer to dimensionless groups where $\tau = T_i/T_2$ and $\sigma = T_e/T_2$. The fact that analysis predicts an extensive hot electron region ahead of the region in which abrupt changes occur in ion velocity (shock within shock) is interesting and may help explain some of the electron precursor observations found in the laboratory. On the other hand, in the real situation radiation, and at times magnetic fields, must also be considered.

Jaffrin and Probstein's results are quite plausable if one thinks of a two-fluid shock as being two separate shocks coupled by electrostatic and dissipative forces. For $T_i \approx T_e$, the electron gas Mach number is less than the ion gas Mach number, and in fact, the electron gas may be subsonic while the ion gas is supersonic. Thus, the ion shock thickness should be less than the electron shock, and the temperature jump of the ion shock should be greater than that in the electron gas. The two gases will relax toward the same final equilibrium temperature and these expected qualitative features are well illustrated in Fig. 6.

The fact that the Navier–Stokes equations are used to study shock structure has been criticized because the length scales are of the order of a mean free path. Nevertheless, in many cases the Navier–Stokes solution serves as an excellent model and gives reasonably good estimates of the mean flow quantities as discussed by Sherman and Talbot (29). Other plasma shock studies have been made by Jukes (30), Shafranov (31), Greenberg *et al.* (32, 33), and Grewal and Talbot (34). Recently, Jaffrin (35) extended (27) and treated a partially ionized gas, but in the analysis he neglects the change in the degree of ionization in the shock structure.

The determination of the actual structure of an ionizing shock is a very difficult and complicated problem since it involves chemical reaction rates (dissociation and ionization rates) as well as the usual gas dynamic and electrodynamic phenomena. However, models of solutions have been set forth by Lyubimov and Kulikovskii (1), Chu (8), May and Tendys (36), and Petcheck and Byron (135). All these models have the similar feature that the electrical conductivity of the gas is assumed to be zero in the pre-shock gas and it continues to be zero in the shock structure until a value T^* is reached by the temperature. At this point in the shock structure the conductivity jumps to a high value σ^* which remains constant through the remainder of the shock wave. The analogy with ignition temperature in flame structure problems is evident.

An idealized structure for an ionizing transverse shock wave is shown in Fig. 7, which is the U–B plane or phase plane. If the thermal conductivity is considered to be zero, then the energy equation is an algebraic equation, and the shock layer is governed by only two differential equations of the form

$$du/dx = f(u, B)$$

$$dB/dx = \sigma g(u, B).$$

The downstream point 2, occurs at the intersection of the curves $f(u, B) = 0$ and $g(u, B) = 0$ and is a saddle point. The upstream 1, may lie anywhere along the curve $f(u, B)=0$ since $\sigma=0$ upstream. To obtain the correct upstream point we follow the structure curve (which will be identical to a hydromagnetic structure curve) out of the singularity 2, until it intersects the curve $T(u, B)=T^*$ which is obtained from the energy equation. Upstream of this point, the value of B remains constant, since the gas is nonconducting. Thus, we now follow a B=constant line until it intersects the curve $f(U, B)=0$. This uniquely determines the upstream point 1 and the corresponding value of the electric field E_1. The problem of a transverse ionizing shock wave is thus, in principle, understood. The real case where the electrical conductivity is a continuous variable and the ionization rates must be taken into account is clearly a much more complicated problem.

V. RADIATIVE SHOCK WAVES

The importance of the radiation energy content of a gas as compared to its internal kinetic energy can be very roughly gauged by the dimensionless parameter ϵ defined as

$$\epsilon=aT^3/nk, \tag{16}$$

where a is the Stefan–Boltzmann radiation density constant, (7.62×10^{-15} ergs/cm^3 °K^4), T the temperature (°K), n the particle number density, and k is the Boltzmann constant (1.38×10^{-16} erg/°K). The parameter ϵ is the ratio of the radiative energy density per unit volume aT^4 to the kinetic internal energy per unit volume of an ideal monatomic gas which is proportional to nkT. When ϵ is of the order of unity, radiation must be included in the shock wave momentum and energy jump equations. The use of ϵ as a gauge implies local thermodynamic equilibrium, including radiation, a situation that often is physically nonrealistic. Nonequilibrium radiative processes are often important in the direct transfer of energy from one fluid volume to another. Their relative importance, compared to thermal convection and conduction, cannot be determined in a simple manner. The appropriate differential equations must first be solved. However certain simple cases can be investigated.

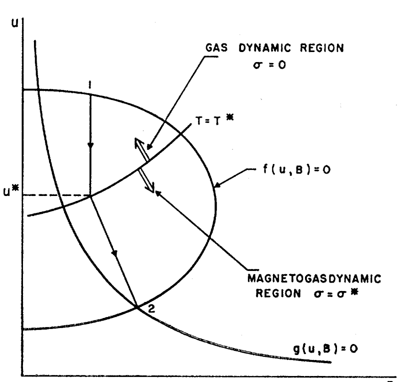

FIG. 7. Phase plane ionizing wave shock structure.

The shock wave jump equations for radiative shocks were first given in the special case of very strong shocks by Sacks (37) and under nonsteady conditions by Guess and Sen (38). Analysis of radiative transfer in the shock problem divides itself naturally into three classes; the optically thick, the optically thin, and the intermediate case. The optical depth of a gas is a function of the length of the photon mean free path which in turn depends on the absorption and scattering properties of the medium. The photon mean free path is strongly dependent on frequency. An optically thick shock is one whose shock thickness is large compared to the photon mean free path.

The subject of radiative shock structure has been studied since 1952, when Prokof'ev (39) in the USSR and later Clarke (40) in the USA considered the case of a steady flow with zero viscosity and zero thermal conductivity. The usual shock discontinuity was altered by "radiation smoothing." Each of the two papers contains an error. Prokof'ev's work was corrected by Zel'dovich (41) and Clarke's work was corrected by Heaslet and Baldwin (42) when a more careful treatment was made of the discontinuous nature of the flow. Heaslet and Baldwin showed that for some physical conditions discontinuities necessarily arise in the temperature and velocity profiles and that strong shocks can exhibit a temperature maximum considerably larger than that corresponding to the Rankine–Hugoniot conditions. In Fig. 8 are shown some of the results on radiation smoothed shocks from the work of Heaslet and Baldwin. Mitchner and Vinokur (43) studied the effect of a magnetic field on a radiating MHD shock and showed that a transverse field will inhibit the smoothing tendency of radiation energy transfer and also alter the conditions for occurrence of a temperature overshoot.

The effect of radiation upon normal shock structure, i.e., where viscosity and thermal conduction are nonzero, were studied by Marshak (44), Traugott (45), and Scala and Sampson (46) in the thin (transparent) and thick (highly absorptive) cases. The influence of radiation on shock structure has been studied as it effects shock tube phenomenon by Pomerantz (47). Whitney and Skalafuris (48) have examined the effect of Lyman continuum radiation on shock waves in stellar atmospheres. Propagating fronts with shock-like properties caused by absorption of radiation in astrophysical phenomena have been studied by Goldsworthy (49) and Axford (50, 51). Koch (52) has recently given a complete solution for shocks in optically thick atmospheres.

A. The Optically Thick Case

Koch's (52) solution of the optically thick shock structure problem assumes that the radiation intensity is attenuated by absorption rather than scattering, and that the atmosphere is in local thermodynamic equilibrium; i.e., Kirchoff's law of radiation applies.

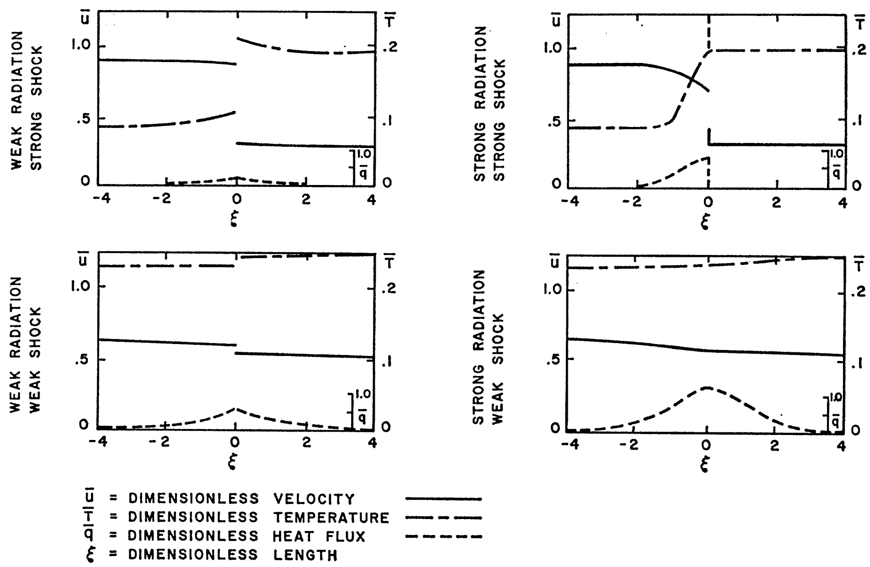

FIG. 8. Radiation smoothed shocks.

The photon mean free path for absorption $L_R{}^a$ is defined by

$$L_R{}^a = 1/n\sigma^a. \tag{17}$$

n is the particle number density, and σ^a is the Rosseland mean absorption coefficient defined as

$$\sigma^a = \int_0^\infty \frac{\partial B_\nu(T)}{\partial T}\, d\nu \Big/ \int_0^\infty \sigma_\nu{}^{-1a} \frac{\partial B_\nu(T)}{\partial T}\, d\nu, \tag{18}$$

where $B_\nu(T)$ is the Planck blackbody function. Menzel and Pekeris (53) gave the absorption coefficient per ionized hydrogen atom as

$$\sigma_\nu{}^a = \frac{C_0 p_e}{\nu^3 T^{\frac{1}{2}}}\left(\exp\left(\frac{h\nu}{kT}\right) - 1\right)\left[1 - 0.1728\left(\frac{\nu}{R_0}\right)^{\frac{1}{3}}\left(1 - \frac{2kT}{h\nu}\right)\right], \tag{19}$$

where $C_0 = 2.67\times 10^{24}$ (cgs units), p_e = electron pressure, ν = frequency, and R_0 = Rydberg constant. Using Eq. (19) in (18) gives

$$\sigma^a = 3.32\times 10^{-7} \frac{p_e}{T^{9/2}}\left[1 - 0.1098\left(\frac{T}{1.57\times 10^5}\right)^{1/2}\right] \text{cm}^2. \tag{20}$$

Equations (17) and (20) permit determination of the photon mean free path which can then be compared with the particle mean free path and hence the relative thickness of an optical atmosphere can be evaluated.

For the optically thick, radiative equilibrium case, the shock jump equations as given by Koch (52), are

$$m[u + (RT/u)] + p_r + \tfrac{1}{2}(\mu H^2) = P, \tag{21}$$

$$Pu + [mRT/(\gamma - 1)] + uU_r - \tfrac{1}{2}(mu^2) + F + EH - \tfrac{1}{2}(\mu u H^2) = Q, \tag{22}$$

$$\mu u H - E = 0, \tag{23}$$

$$l\,(\partial I_\nu/\partial \tau_\nu) = B_\nu(T) - I_\nu, \tag{24}$$

where P and Q are constants, I_ν is the specific radiation intensity, l is the direction cosine, and τ_ν the optical depth at frequency ν. The optical depth τ_ν is defined by,

$$\tau_\nu = \int K_\nu \rho\, dx,$$

where K_ν is the mass coefficient of extinction (sum of absorption and scattering coefficients). The quantities F, U_r, and p_r for radiant flux, radiation energy, and pressure, are defined by

$$F \equiv 2\pi \int_0^\infty d\nu \int_{-1}^{1} l I_\nu\, dl, \tag{25}$$

$$U_r \equiv \frac{2\pi}{c} \int_0^\infty d\nu \int_{-1}^{1} I_\nu\, dl, \tag{26}$$

$$p_r \equiv \frac{2\pi}{c} \int_0^\infty d\nu \int_{-1}^{1} l^2 I_\nu\, dl. \tag{27}$$

These quantities for the special case of radiative equilibrium pre- and post-shock states are given by

$$F = 0, \tag{25a}$$

$$U_r = aT^4/p, \tag{26a}$$

$$p_r = \tfrac{1}{3}(aT^4/p). \tag{27a}$$

The seven equations [(21)–(24), (25a)–(27a)] can be combined into a single twelfth-order polynomial in the variable ω where $\omega = mu/p$. This equilibrium radiative shock equation has been analyzed in detail and solved by Koch (52). He shows that there are only two physically real roots corresponding to the usual pre- and post-shock states. The resulting post-shock temperature is shown in Fig. 1 as the right-hand branching curve which departs from the nonradiative solution at a temperature $T \approx 10^5$ °K corresponding to a shock wave speed of about 10^5 m/sec. The slope of the radiative equilibrium temperature vs wave speed is much less than the nonradiative case.

The density ratio for radiative equilibrium shocks is shown in Fig. 2 as the branch of the curve beginning at $u_1 \approx 10^5$ m/sec and which is asymptotic to $\rho_2/\rho_1 = 7.0$. This asymptotic result agrees with the fact that a photon gas behaves as if it were a gas with a specific heat ratio $\gamma = \frac{4}{3}$ (54) and the density ratio for a strong shock is given by the well-known result,

$$\rho_2/\rho_1 = (\gamma+1)/(\gamma-1) = 7 \quad \text{for photon gas} \quad \gamma = \tfrac{4}{3}. \quad (28)$$

The speed of propagation of a small disturbance through a gas consisting of electrons, protons, and photons in complete equilibrium is

$$v^2 = \gamma' RT, \quad (29)$$

where

$$\gamma' = 1 + \{(1+\tfrac{4}{3}\epsilon)^2/[(\gamma-1)^{-1}+4\epsilon]\} \quad (30)$$

and ϵ is the radiation parameter defined by Eq. (16). Equation (29) is like the familiar small disturbance speed in an ideal gas except the effective γ shows the influence of radiation. It can be shown that, employing the results of Eqs. (29) and (30), the post-shock states in radiative equilibrium shocks are always moving at subsignal speeds and there is always an increase of entropy.

Koch has also studied numerically the structure of such radiative equilibrium shocks under the assumption that the Eddington approximation (photon diffusion) is valid. Such shocks are extremely thick (in excess of 10^4 meters) and hence these solutions are of little interest for laboratory shock experiments. They may, however, occur in astrophysical cases. Two radiatively thick shock structure curves are shown in Fig. 9.

B. The Optically Thin Case

For nearly all laboratory-produced shock wave situations the photon mean free path over most of the frequency spectrum is much larger than the size of the experiment. Consequently nearly all photons emitted by the hot plasma escape from the plasma to the surrounding walls. This represents a time-dependent energy loss from the plasma and there is no true steady-state reference frame for shock structure analysis. There will be, however a temperature maximum in the optically thin case which can be compared with the equilibrium post-shock state previously calculated for the same initial state and wave speed. (See, for example, Fig. 10.) Cohen and Clarke (133) have shown that there is an imbedded viscous heat-conducting shock identical in structure to a shock without radiation but for different initial and final states.

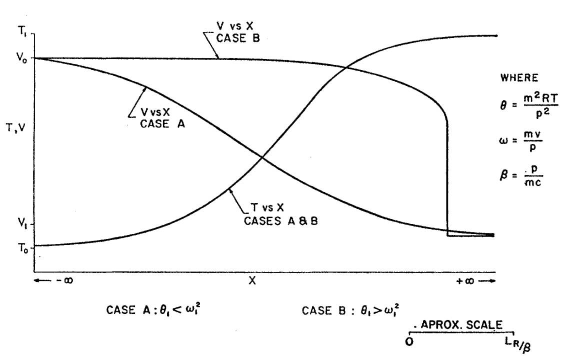

FIG. 9. Optically thick shock structure.

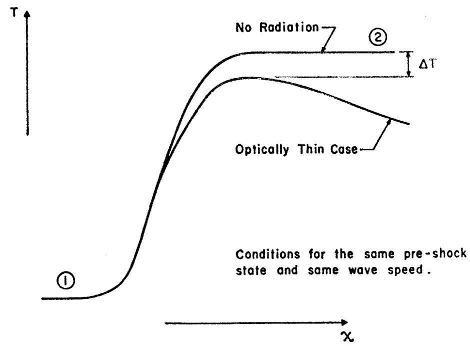

FIG. 10. Optically thin shock structure.

Consider 1 and 2 to be the upstream and downstream states relative to a strong gas dynamic shock in hydrogen with radiation ignored. During the transition between these two states an amount of energy ΔE is assumed to be totally lost from the gas due to radiation into an optically thin atmosphere. This loss of energy has the effect of lowering the maximum downstream temperature by an amount.

$$\Delta T = \Delta E/\rho_2 C_v. \quad (31)$$

Such analysis is valid so long as $\Delta T/T_1 \ll 1$; i.e., the radiation loss is a perturbation on the nonradiative shock problem.

The gas is assumed to radiate according to bremstrahlung .Thus,

$$dE/dt = 1.57\times10^{-27} n^2 T^{\frac{1}{2}} \text{ (ergs/cm}^3\text{ sec)}, \quad (32)$$

where E is the energy per unit volume and n is the number of charged particles per cubic centimeter. The energy loss is

$$\Delta E = \int_1^2 \frac{dE}{dt}\, dt = 1.57\times10^{-27}\int_1^2 n^2 T^{\frac{1}{2}}\, dt, \quad (33)$$

where the integration must be performed along the shock structure curve given by $n = n(x)$; $T = T(x)$. For each particle, the time element is

$$dt = dx/u(x), \quad (34)$$

where $u(x)$ is the velocity of the gas relative to the shock. The energy loss is

$$\Delta E = 1.57\times10^{-27}\int_1^2 \frac{n^2 T^{\frac{1}{2}}}{u(x)}\, dx \quad (35)$$

and the temperature defect,

$$\Delta T = \frac{1.57\times10^{-27}}{\rho_2 C_v}\int_1^2 \frac{n^2 T^{\frac{1}{2}}}{u(x)}\, dx. \quad (36)$$

If the chemistry of dissociation and ionization in

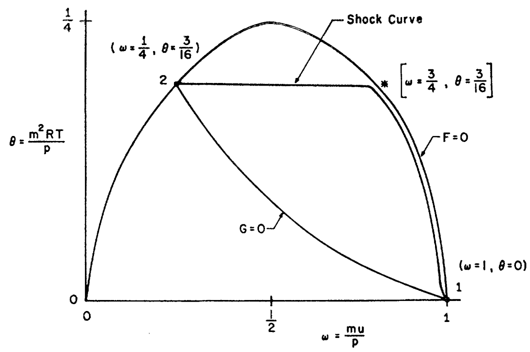

FIG. 11. Phase plane optically thin shock structure.

the leading edge of a strong radiating shock wave is ignored, then mass conservation is given simply by

$$nu=\text{constant}=m/m_H=\rho u/m_H, \tag{37}$$

where m is the mass flow constant of Eq. (2) and m_H is the hydrogen ion mass. Therefore,

$$\Delta T=\frac{1.57\times10^{-27}}{C_v}\frac{u_2m}{m_H^2}\int_1^2\frac{T^{\frac{1}{2}}}{u^3}\,dx. \tag{38}$$

To estimate the temperature defect predicted by Eq. (38) the shock structure curve was approximated by the following simple linear equations

$$T=T_1+(T_2-T_1)(x/t_\theta) \tag{39}$$

$$u=u_1-(u_1-u_2)(x/t_\omega), \tag{40}$$

where t_θ and t_ω are the shock thicknesses with respect to temperature and velocity, respectively. By definition,

$$t_\theta=|T_2-T_1|/|dT/dx|_{\max} \tag{41}$$

$$t_\omega=|u_1-u_2|/|du/dx|_{\max}. \tag{42}$$

The shock structure equations can be put into the dimensionless form [following Koch (52)]

$$L_p\,(d\omega/dx)=\omega+(\theta/\omega)-1=F(\omega,\theta) \tag{43}$$

$$L_H\,(d\theta/dx)=\theta-\tfrac{1}{3}[(1-\omega)^2+A]=G(\omega,\theta), \tag{44}$$

where $L_p=4\eta/3m$ and $L_H=K/Cum$ are the momentum and energy transfer characteristic lengths, respectively, and η and K are the viscosity and thermal conductivity of the gas. The shock strength constant A in Eq. (44) is defined by $A=(20m/p^2)-1$. The dimensionless velocity ω and temperature θ are defined by,

$$\omega=mu/p \tag{45}$$

$$\theta=m^2RT/p^2. \tag{46}$$

Then

$$|d\omega/dx|_{\max}=|F|_{\max}/\bar{L}_p \tag{47}$$

$$|d\theta/dx|_{\max}=|G|_{\max}/\bar{L}_H, \tag{48}$$

where barred quantities are averaged over the shock structure curve. It can be shown (51) that $\bar{L}_H\gg\bar{L}_p$ for an ionized gas so that the shock structure curve will follow the curve $F=0$ near the pre-shock state. Since only very strong shocks are considered, it is appropriate to set $A\approx0$ so that the structure of the shock wave, as viewed in the phase plane appears as shown in Fig. 11.

Along the shock structure curve as shown in Fig. 11, the maximum value of F will occur along the horizontal line $\theta=\frac{3}{16}$. Therefore,

$$F=\omega+(3/16\omega)-1$$

$$dF/d\omega=1-(3/16\omega^2)\qquad\omega_{\max}=0.433. \tag{49}$$

Therefore,

$$|F|_{\max}=0.134. \tag{50}$$

The maximum value of G can occur either along that line or along the curve $F=0$. On the former,

$$G=\tfrac{3}{16}-\tfrac{1}{3}(1-\omega)^2$$

$$dG/d\omega=\tfrac{2}{3}(1-\omega) \tag{51}$$

so that the maximum value of G along that line is at the point marked * in Fig. 11 ($\omega=\frac{3}{4}$, $\theta=\frac{3}{16}$), where $G=\frac{1}{6}$. Along the curve $F=0$, it can be shown that the maximum occurs at $\omega=\frac{5}{8}$ which is not on the shock curve. Therefore,

$$|G|_{\max}=0.167. \tag{52}$$

Then

$$t_\omega=(0.750/0.134)\,L_p=5.60\bar{L}_p$$

$$t_\theta=\tfrac{3}{16}L_H/\tfrac{1}{6}=1.125\bar{L}_H.$$

For an ionized hydrogen gas $\bar{L}_H\approx80\bar{L}_p$ and $t_\theta\approx90\bar{L}_p$. The expression for L_p is

$$L_p\approx\frac{0.5097\times10^{-14}}{m}\frac{T^{5/2}}{\ln[0.547\times10^9(T^3/n)]}. \tag{53}$$

For simplicity, the denominator of Eq. (53), a slowly varying function of T and u, can be replaced by $\ln(0.547\times10^9\,\bar{T}^3/n_1)$ where $\bar{T}$ is some reasonable mean shock temperature. Then,

$$\bar{L}_p=\frac{0.5097\times10^{-14}}{m\ln[0.547\times10^9(\bar{T}^3/n_1)]}\times\int_{t_{\theta_1}}^{t_0}\left[T_1+(T_2-T_1)\frac{x}{t_\theta}\right]^{5/2}dx. \tag{54}$$

The amount the shocked gas temperature maximum is reduced by bremstrahlung can now be evaluated using Eqs. (38), (39), (40), and (54). This has been done numerically for the given initial hydrogen state and the result is shown in Fig. 1. The maximum temperature as indicated in Fig. 10 for the optically thin case is nearly identical to the nonradiative solution up to a wave speed of about 10^7 m/sec ($T_2\approx10^9$ °K). The effect becomes more pronounced as the shocked gas temperature increases and the approximation is most probably not valid above about 10^{10} °K.

A very interesting study of the structure of a shock front in atomic hydrogen has been carried out by Whitney and Skalafuris (48). They examined the effects of the Lyman continuum radiation that passes through the shock front and that is absorbed in the pre-shock gas. They showed that electrons produced in the pre-shock gas by Lyman continuum radiation do not recombine before passing through the shock front. They concentrate on the thermal structure of a radiating shock, neglecting all effects of viscosity, thermal conduction and electric and magnetic fields. They also point out that for shocks where $T_2 < 10^5$ °K free–free radiation contributes only one-fourth as much as free–bound radiation. The bound–bound emission in the Lyman spectrum can be neglected since their total energy content is small and this radiation will be trapped in the hot product gas (which is optically thick for these lines). Whitney and Skalafuris also show that the pre-shock gas is significantly heated and ionized by the precursor radiation. However, their temperature boundary conditions are not the usual ones, but are more relevant to stellar problems.

VI. RELATIVISTIC SHOCK WAVES

The theoretical foundations of relativistic shock waves have been studied by Eckart (55), Taub (56), Landau and Lifshitz (57), Synge (58), etc. The relativistic magnetohydrodynamic shock has been studied by De Hoffman and Teller (59) and Kovrezhnykh (60). It seems certain that radiation also must play an important role in such very fast shocks.

Following Synge (58), e, the energy per unit volume, and p, the pressure of a nonradiating relativistic monatomic gas in its proper reference frame, are given by

$$e+p=\rho c^2 G(\alpha) \tag{55}$$

$$p=\rho c^2/\alpha, \tag{56}$$

where ρ is the proper density, c the velocity of light, and α is the reciprocal dimensionless temperature defined by

$$\alpha=c^2/RT.$$

R is the gas constant and T is the absolute temperature. $G(\alpha)$ is a function which can be approximated by

$$G(\alpha)=1+5/2\alpha \qquad \text{for} \quad \alpha \geq \tfrac{3}{2}$$

$$G(\alpha)=4/\alpha \qquad\qquad \alpha \leq \tfrac{3}{2}. \tag{57}$$

For ionized hydrogen, Eqs. (55) and (56) are replaced by

$$e+p=\rho c^2 Q(\alpha) \tag{58}$$

$$p=2\rho c^2/\alpha, \tag{59}$$

where

$$Q(\alpha)=G(\alpha)+\delta G(\alpha) \tag{60}$$

and $\delta=m_e/m_H$, the ratio of electron to proton mass. If equilibrium radiation is assumed, the energy and pressure are given by

$$e+p=\rho c^2 Q(\alpha)+\tfrac{4}{3}aT^4 \tag{61}$$

$$p=(2\rho c^2/\alpha)+\tfrac{1}{3}aT^4 \tag{62}$$

or

$$e+p=\rho c^2[Q+\tfrac{4}{3}(\epsilon/\alpha)] \tag{63}$$

$$p=(\rho c^2/\alpha)(2+\tfrac{1}{3}\epsilon), \tag{64}$$

where

$$\epsilon=aT^3/\rho R$$

$$\epsilon/\alpha=aT^4/\rho c^2.$$

The relativistic shock jump equations are (see e.g., Ref. 56)

$$n_1\beta_1\gamma_1=n_2\beta_2\gamma_2, \tag{65}$$

$$\beta_1\gamma_1^2(e_1+p_1)=\beta_2\gamma_2^2(e_2+p_2), \tag{66}$$

$$(e_1+p_1)\beta_1^2\gamma_1^2+p_1=(e_2+p_2)\beta_2^2\gamma_1^2+p_2, \tag{67}$$

where $\beta=u/c$, $\gamma=(1-\beta^2)^{-\frac{1}{2}}$, u = velocity relative to the shock, and n = particle number density. For a neutral singly ionized gas $n=n_i=n_e$ and $\rho=n_im_i$. Equations (65), (66), and (67) can be combined algebraically into

$$\left(\frac{\rho_2}{\rho_1}\right)^2=\left(\frac{\beta_1\gamma_1}{\beta_2\gamma_2}\right)^2=\frac{e_2+p_2}{e_1+p_1}\cdot\frac{e_2+p_1}{e_1+p_2} \tag{68}$$

Using Eqs. (63) and (64) the density ratio is

$$\frac{\rho_2}{\rho_1}=\left(Q_2+\frac{4}{3}\frac{\epsilon_2}{\alpha_2}\Big/Q_1+\frac{4}{3}\frac{\epsilon_1}{\alpha_1}\right)\cdot\left\{\left(\frac{\rho_2}{\rho_1}\right)\left[Q_2+\frac{\epsilon_2}{\alpha_2}-\frac{2}{\alpha_2}\right]+\frac{2+\frac{1}{3}\epsilon_1}{\alpha_1}\right\}\Big/\left[Q_1+\frac{\epsilon_1}{\alpha_1}-\frac{2}{\alpha_1}+\left(\frac{\rho_2}{\rho_1}\right)\frac{2+\frac{1}{3}\epsilon_2}{\alpha_2}\right]. \tag{69}$$

If the initial gas state is cold, then it is appropriate to assume that

$$\alpha_1 \gg \tfrac{3}{2}, \qquad p_1 \ll e_1 \quad \text{and} \quad \epsilon_1 \ll 1$$

so that Eq. (69) reduces to

$$1=\left[\left(Q_2+\frac{4}{3}\frac{\epsilon_2}{\alpha_2}\right)\left(Q_2+\frac{\epsilon_2}{\alpha_2}-\frac{2}{\alpha_2}\right)\right]\Big/\left[1+\frac{\rho_2}{\rho_1}\left(\frac{2+\frac{1}{3}\epsilon_2}{\alpha_2}\right)\right]. \tag{70}$$

As for the final shock state, the energy and pressure terms are of three orders, namely, $O(1)$, $O(\epsilon_2/\alpha_2)$, and $O(\alpha_2)^{-1}$ in descending order. If terms of $O(\alpha_2)^{-1}$ can be ignored, Eq. (70) reduces to

$$\rho_2/\rho_1=(2+\tfrac{1}{3}\epsilon_2)^{-1}\{8+\tfrac{1}{3}\epsilon_2[7+\tfrac{4}{3}(\epsilon_2/\alpha_2)]\}. \tag{71}$$

If $\epsilon_2=0$ (nonradiative case), the result $\rho_2/\rho_1=4$ is the same as for strong shocks in a monatomic gas. If $\epsilon_2 \gg 1$ then

$$\rho_2/\rho_1=7+(4\epsilon_2/\alpha_2) \tag{72}$$

and if (ϵ_2/α_2) can be ignored, the density ratio is 7, the same result for equilibrium radiative shocks with relativistic effects ignored.

The velocity ratio can be obtained from Eq. (66).

Thus,

$$\frac{\gamma_1}{\gamma_2}=\frac{\beta_2\gamma_2}{\beta_1\gamma_1}\cdot\frac{e_2+p_2}{e_1+p_1}=\left(\frac{\rho_1}{\rho_2}\right)\frac{e_2+p_2}{e_1+p_1} \tag{73}$$

or

$$\frac{\gamma_1}{\gamma_2}=\frac{Q_1+\frac{4}{3}(\epsilon_2/\alpha_2)}{Q_1+\frac{4}{3}(\epsilon_1/\alpha_1)}=1+\frac{4}{3}\frac{\epsilon_1}{\alpha_1}. \tag{74}$$

Equations (72) and (74) together with the definitions of β and γ are sufficient to determine the four quantities β_1, β_2, γ_1, and γ_2 in terms of the parameter ϵ_2/α_2. Specifically, let

$$\zeta=\gamma_1/\gamma_2$$

$$\nu=(\rho_2/\rho_1).$$

Then,

$$\gamma_1^2=\zeta^2(\nu^2-1)/(\nu^2-\zeta^2), \tag{75}$$

$$\beta_1^2=\nu^2(\zeta^2-1)/\zeta^2(\nu^2-1), \tag{76}$$

$$\gamma_2^2=(\nu^2-1)/(\nu^2-\zeta^2), \tag{77}$$

$$\beta_2^2=(\zeta^2-1)/(\nu^2-1). \tag{78}$$

The final temperature behind a shock, for given initial gas conditions can be determined as a function of shock speed. A numerical procedure was employed by assuming a value of $\epsilon_2/\alpha_2=aT_2^4/\rho_2c^2$ and then solving for the final state. Thus,

$$\nu=\rho_2/\rho_1=7+(4\epsilon_2/\alpha_2),$$

$$\rho_2=\nu\rho_1,$$

$$T_2=[(\rho_1c^2/a)\cdot(\epsilon_2/\alpha_2)]^{\frac{1}{4}},$$

$$\zeta=1+\tfrac{4}{3}(\epsilon_2/\alpha_2),$$

$$\beta_1=(\nu/\zeta)[(\zeta^2-1)/(\nu^2-1)]^{\frac{1}{2}},$$

and

$$u_1=\beta c.$$

The results can be seen in Figs. 1 and 2 for velocities above about 10^8 m/sec.

Relativistic shocks occur in astrophysics. The interest in shock waves in astrophysics is evident from the works of Masani (61), Whitney and Skalafuris (48), Schwartzschild (62), Kaplan and Klimishin (63), Goldsworthy (49), Axford (50, 51), Colgate (131, 132), etc. It is interesting to note that present day laboratory experiments with electromagnetic shock tubes are generating conditions very close to those in some astrophysical cases. For example, Whitney and Skalafuris (48) analytically studied shocks moving at 5×10^4 m/sec into hydrogen with $n_1\approx10^{15}$ cm^{-3} as representative of observed shocks on W Virginis.

Very strong shocks may generate a gas whose temperature is of the order of the rest mass of the electron ($kT\approx m_ec^2=0.51\times10^6$ eV$=6\times10^9$ °K). Such a gas will exhibit pair production where collisions create electrons and positrons. Thus

$$e^++e^-=\gamma \quad \text{(one or several photons)}.$$

Once again, number density is no longer conserved and, somewhat analogous with slow speed shocks where dissociation and ionization are important, very high speed shocks have their particular high-energy chemistry. For the equilibrium case Landau (64) has shown that for,

$$kT\ll mc^2 \qquad n^+=n^-=4(mkT/2\pi\hbar)^3\exp(-2mc^2/kT),$$

$$kT\gg mc^2 \qquad n^+=n^-=0.183(kT/\hbar c)^3,$$

and

$$E^+=E^-=[7\pi^2(kT)^4/120(\hbar c)^2]V,$$

where n^+ of the positron number density and E^+ is the positron energy in a volume V. It is interesting to note that E^+ is seven-eighths the energy of blackbody radiation in the same volume.

VII. THERMONUCLEAR SHOCKS

If the initial gas state consists of deuterium or tritium, the isotopes of hydrogen, it is possible to obtain an exothermal strong shock wave where energy is released by thermonuclear reactions. The thermonuclear shock problem requires solution of the fusion shock wave structure to assure that the fusion requirements of sufficient particle energy, density, and residence time are satisfied. Assuming these criteria are satisfied, the jump conditions across the wave can be easily solved. Since the post-shock state must be of the order of 10^{10} °K, the strong shock approximations are certainly valid.

The simplest set of relevant shock jump equations are

$$\rho_1u_1=\rho_2u_2, \tag{79}$$

$$p_1+\rho_1u_1^2=p_2+\rho_2u_2^2, \tag{80}$$

$$\tfrac{1}{2}u_1^2+C_pT_1+Q=\tfrac{1}{2}u_2^2+C_pT_2. \tag{81}$$

The value of Q in Eq. (81) is taken for a pure deuterium gas in which there is complete burnup. All the following reactions take place (65):

$$\begin{aligned}
&\mathrm{D+D} &&\rightarrow \mathrm{T}(1.0\ \mathrm{MeV})+p(3.0)\\
&\mathrm{D+D} &&\rightarrow \mathrm{He}^3(0.8)+n(2.45)\\
&\mathrm{D+T} &&\rightarrow \mathrm{He}^4(3.5)+n(14.1)\\
&\mathrm{D+He}^3 &&\rightarrow \mathrm{He}^4(3.6)+p(14.7)\\
\hline
&6\mathrm{D} &&\rightarrow 2\mathrm{He}(7.1)+2p(17.7)+2n(16.55)+1.8\,.
\end{aligned}$$

The average energy of the six deuterons is 7.1 MeV and the energy released per gram of deuterium (for complete burnup) is $Q_{\mathrm{DD}}=3.59\times10^{18}$ erg/g. The value of Q for a deuterium–tritium mixture is also about equal to this value.

Solving Eqs. (79), (80), and (81) for the product gas temperature in the strong shock limit yields

$$RT_2=\frac{2(\gamma-1)}{\gamma+1}Q+\frac{(\gamma-1)u_1^2}{(\gamma+1)^2}\left\{1\pm\left[1-2(\gamma^2-1)\frac{Q}{u_1^2}\right]^{\frac{1}{2}}\right\}. \tag{82}$$

This type of exothermal shock wave solution has been extensively studied for detonations where the energy release is supplied by chemical reactions. The post-shock state for a thermonuclear reaction is shown in Fig. 1. There is no steady-state solution for values of $u_1 < 3.56\times 10^7$ m/sec which is the singular point for a DD thermonuclear shock. (i.e., the square root in Eq. (82) is equal to zero). For speeds greater than that of the singular point, there are two solutions to the conservation equations. These are the so-called strong and weak wave solutions. The strong wave solution, which parallels the ordinary shock solution in Fig. 1 is characterized by subsonic flow in the post-shock state. The weak solution has supersonic flow behind it while the singular point, $u_1=3.56\times 10^7$ m/sec, has sonic post shock flow, namely $u_2/a_2=1$. The density ratio for a thermonuclear shock wave is shown in Fig. 2. It is generally regarded that the weak branch is physically unstable.

The properties of waves in magnetohydrodynamics which release or absorb energy have been studied by Barmin (66). This is a natural extension to the well developed gas dynamic literature which treats chemical reactions in fluid flow, such as deflagrations, detonations, etc.

VIII. THE SHOCK TUBE PROBLEM

The history and development of the shock tube as a source of strong shock waves has recently been reviewed and summarized by Kantrowitz (67). The coaxial electromagnetically driven shock tube as pioneered by Patrick (68) has helped open up the highly ionized, strong shock regime. Kemp and Petschek (69) have analyzed the behavior of the flow in a coaxial electromagnetically driven shock tube under the assumptions of large electrical conductivity and no chemistry. Their solution is valid if the pre-shock gas is completely ionized and the magnetohydrodynamic assumption of infinite electrical conductivity is implied. The shocks produced in T tubes, cylindrical shocks, etc., are usually nonsteady waves and they are discussed in detail by Kolb and Griem (70).

The corresponding problem for the more realistic experimental case of ionizing shock waves, where the

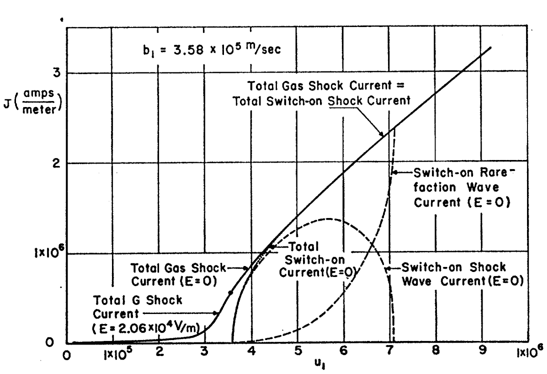

FIG. 12. Shock tube current vs wave speed.

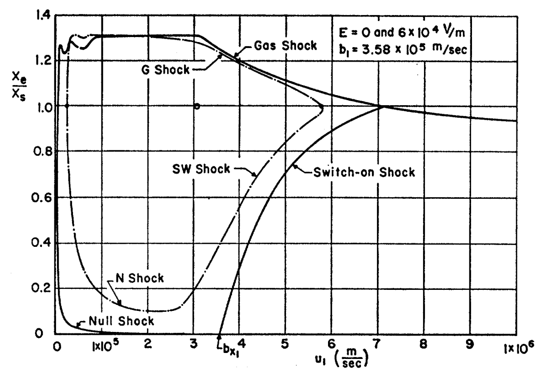

FIG. 13. Expansion-wave–shock-wave speed ratio (chemical equilibrium).

dissociation and ionization at the wave front is important, has been solved numerically by Taussig (10). The configuration studied is shown in Fig. 4. The electrical current required to drive an ionizing shock wave at a speed u_1 is shown in Fig. 12 from the work of Taussig. In Fig. 1 are shown some drive currents required to develop the shock velocities shown. The current J (ampere/meter) refers to the total electric current per meter of circumferential length of the shock tube. The current is completely confined to the expansion wave except during switch-on behavior in which case some current also passes through the shock wave structure. In Fig. 12 is shown the total current and rarefaction wave current for the switch-on regime.

For a steady shock to exist it must move faster than the slow expansion wave. The ratio of their speeds is given by the ratio x_e/x_s, the expansion distance to shock wave distance traveled during a given time t. The value of x_e/x_s is shown in Fig. 13 for the chemical equilibrium ionizing wave computed by Taussig (10). It is important to note that values of $x_e/x_s>1$ represent nonsteady solutions. That is, the expansion wave moves faster than the shock wave and continually decreases the post-shock state and hence the speed at which the shock travels. For slow ionizing waves, except for the N shock class of solutions, there is no steady-state shock tube problem solution. For shock wave speeds equal to or greater than the switch-on speed, there are steady solutions to the electromagnetic shock tube problem as shown in Fig. 9 where there are solutions where $x_e/x_s\leq 1$.

Various aspects of the electromagnetic shock tube have been studied with emphasis on circuit parameters and how they influence the wave speed. For example, Wright and Black (71) studied the acceleration phase of an electromagnetically driven shock wave and Hart (72) studied the variable inductance of a shock wave as it propagates along a coaxial geometry. Wright and Black show that for typical experimental devices with fast-rise-time current pulses, the acceleration phase should be essentially over when the circuit inductance has increased to three times its initial value. This corresponds to a relatively short distance in a typical shock tube. The variable inductance created by the wave traveling down the shock tube is an example of Lenz's law. Extremely fast waves develop an inductance which limit the current rise time and hence limit the maximum velocity that may be achieved in such devices.

IX. ASYMPTOTIC FORMULAS FOR VERY FAST GAS SHOCKS JUMP CONDITIONS

For shock speeds in hydrogen greater than about 10^5 m/sec, the post-shock state is completely ionized. If it is assumed that the shock Mach number $u_1/a_1 \gg 1$ and the post-shock is completely ionized, then algebraic solutions to the shock jump equations and the electromagnetic shock tube problem can be explicitly given. Thus, the post-shock pressure is

$$p_2=\tfrac{1}{2}\left(\frac{2(\alpha_2-1)}{2\alpha_2-1}(p_1+\rho_1u_1^2)+\left[\left(\frac{2(\alpha_2-1)}{2\alpha_2-1}(p_1+\rho_1u_1^2)\right)^2 -\frac{4}{(2\alpha_2-1)}\{\rho_1u_1^2p_1[2(\alpha_1-1)-g]-p_1^2\}\right]^{\frac{1}{2}}\right), \quad (83)$$

where

$$g=\frac{2}{T_1}\left(\frac{2\chi}{k}+\frac{\psi}{k}\right);$$

χ = ionization energy per particle: ψ = dissociation energy per particle; k = Boltzmann constant; and $\alpha_i=\gamma_i/\gamma_i-1$, where $i=1$, 2, for pre- and post-shock states. If $\gamma_1=\frac{7}{5}$ and $\gamma_2=\frac{5}{3}$, then

$$p_2=\tfrac{1}{2}\left(\tfrac{3}{4}(p_1+\rho_1u_1^2)+\{[\tfrac{3}{4}(p_1+\rho_1u_1^2)]^2 -\rho_1u_1^2p_1(5-g)+p_1^2\}^{\frac{1}{2}}\right). \quad (84)$$

In the limit of $u_1 \gg a_1$ Eq. (84) reduces to

$$p_2\approx\tfrac{3}{4}\rho_1u_1^2. \quad (85)$$

The mass density ratio is

$$\frac{\rho_2}{\rho_1}=\frac{(p_2/p_1)(2\alpha_2-1)+1}{(p_2/p_1)+(2\alpha_1-1)-g}=\frac{4(p_2/p_1)+1}{(p_2/p_1)+6-g}, \quad (86)$$

and for very strong shocks the well-known result is

$$\rho_2/\rho_1\approx 4. \quad (87)$$

The fluid velocity of the post-shock state, relative to shock fixed coordinates is simply

$$u_2=\rho_1/\rho_2=u_1/4. \quad (88)$$

The post-shock temperature for high-speed gas shocks in hydrogen is

$$T_2/T_1=\tfrac{1}{4}(p_2/p_1)(\rho_1/\rho_2), \quad (89)$$

where the $\frac{1}{4}$ is the ratio of the pre- and post-shock molecular weights.

For initial diatomic hydrogen gas at 273 °K, and $u_1 \gg a_1$

$$T_2\approx 1.14\times 10^{-5}\, u_1^2 \quad T(°\mathrm{K}) \quad u_1\ (\mathrm{m/sec}).$$

In terms of the shock Mach number, these strong shock formulas are

$$p_2/p_1\approx\tfrac{21}{20}M_1^2,$$
$$\rho_2/\rho_1\approx 4,$$
$$u_2/u_1\approx\tfrac{1}{4},$$
$$T_2/T_1=(\tfrac{21}{20})(\tfrac{1}{4}M_1)^2.$$

X. ASYMPTOTIC FORMULAS FOR THE SHOCK TUBE PROBLEM

The results of the shock tube boundary value problem can also be explicitly given in the strong (but non-relativistic) shock limit.

The length of the uniform post-shock gas sample can be estimated easily in the strong shock limit. If X_s is the shock position and X_e is the leading edge of the current rarefaction wave at the time t, then the length of the uniform gas sample is L defined by

$$L=(X_s-X_e).$$

Also,

$$X_s=u_1t.$$

But from the work of Taussig (9),

$$\frac{X_s-X_e}{X_s}=1-\frac{X_e}{X_s}=\frac{[(u_1^2+3a_1^2)^{\frac{1}{2}}-2b_{x1}](u_1^2+3a_1^2)^{\frac{1}{2}}}{4u_1^2}. \quad (90)$$

Therefore,

$$L=\frac{[(u_1^2+3a_1^2)^{\frac{1}{2}}-2b_{x1}](u_1^2+3a_1^2)^{\frac{1}{2}}u_1t}{4u_1^2}. \quad (91)$$

In the strong shock limit of $u_1\rightarrow\infty$ one gets

$$L\approx u_1t/4. \quad (92)$$

It is interesting to note that this strong shock uniform gas sample length is independent of b_x. Let the time that a fluid element remains at uniform post-shock state be $\boldsymbol{\tau}$. Then,

$$\boldsymbol{\tau}=L/u_2=4L/u_1=t. \quad (93)$$

This interesting simple result means that a fluid element swallowed by a very strong shock wave which has been traveling for a time t will remain at a uniform post-shock temperature (neglecting radiation) for a time also equal to t, before entering the rarefaction wave.

A successful thermonuclear fusion reaction needs a number density and containment time product of about

$$n\boldsymbol{\tau}\gtrsim 10^{15}\ \mathrm{sec/cm^3}.$$

It can be seen that a linearly driven shock tube of reasonable length cannot produce fusion. For $n\approx 10^{16}$, a uniform post-shock state of about 0.1 sec is required which means the shock wave must travel for about 0.1 sec. However since a fusion shock wave must travel at $u_1\gtrsim 3\times 10^7$ m/sec, a linear electromagnetic fusion shock tube would have to be longer than 3×10^6 m. Clearly this is not the way to produce fusion in a laboratory.

The electric current needed to drive a very fast gas shock into a quiescent low-pressure monatomic gas with a normal magnetic field H_x will now be estimated. At velocities above $2b_{x1}$ (above the switch-on case) all the current flows through the rarefaction fan. The flow in the expansion wave, which is a slow magnetohydrodynamic expansion wave, is described by the differential equation (Ref. 69)

$$dq/dr=(1-q)r^4q^2/(1-q^2r^5), \tag{94}$$

where $q=(c^s/a)^2$ c^s=slow MHD wave speed. $r=(a/b_x)^{2/5}$. For very high shock velocities, the rear boundary condition terminating the integration of Eq. (94) is $r=0$. This corresponds to a vacuum. The equation for the transverse magnetic field can be shown to be

$$(d/dr)(\mu H_y^2/2)=(q-1)(5p_2)[r^4/(r_2)^5]. \tag{95}$$

At the leading edge of the wave

$$q=q_2=(b_{x2}/a_2)^2=\tfrac{4}{5}(b_{x1}/u_1)^2\ll 1.$$

Also

$$dq/dr]_2=[\tfrac{4}{5}(b_{x1}/u_1)^2]^{6/5}\ll 1.$$

This implies q changes very slowly and in fact decreases as r goes from r_2 to $r=0$ at the end of the rarefaction wave. Therefore it is a good approximation to set $q=0$ everywhere. Thus, the magnetic field pressure across the expansion wave must balance the post-shock gas pressure. This is frequently refered to as the "snow plow" model. Thus,

$$[\mu H_y^2/2]_2^4=p_2=\mu H_y^2/2 \quad \text{and} \quad dq/dr=0,$$

where the superscript 4 represents the post-rarefaction wave state. The electric current J_y per unit circumferential length of shock tube creates the change in the transverse magnetic field between gas state 1 and 4. Thus,

$$J_y/H_x=H_y/H_x=(2p_2/\mu)^{\frac{1}{2}}\cdot(H_x)^{-1}. \tag{96}$$

Since $2p_2=2m(u_1-u_2)=\frac{3}{2}\rho u_1^2$, Eq. (96) can be put in the following convenient form:

$$J_y/H_x=(3/2)^{\frac{1}{2}}(u_1/b_1). \tag{97}$$

XI. STABILITY

The stability and evolutionarity of normal magnetohydrodynamic shocks have been the subject of considerable recent theoretical investigation. These questions for one dimensional disturbances have been summarized in the book by Jeffrey and Taniuti (73) and three dimensional disturbances are considered in the paper by Gardner and Kruskal (74). By stability and evolutionarity is meant the following:

A shock is *evolutionary* if the small perturbation problem linearized about the steady-state (unperturbed) shock has a unique solution. The question of evolutionarity was initially raised by several Soviet writers, notably Akhiezer (75), Syrovatskii (76), and Polovin (77).

A shock is *stable* to small disturbances if the transmitted and reflected disturbances and the perturbed shock velocity remain bounded in time (e.g., do not grow exponentially in time). Stable shocks must be evolutionary, though the converse need not generally be true. Evolutionarity is a subclass of stability in that the disturbances are restricted to plane waves parallel to the plane of the shock.

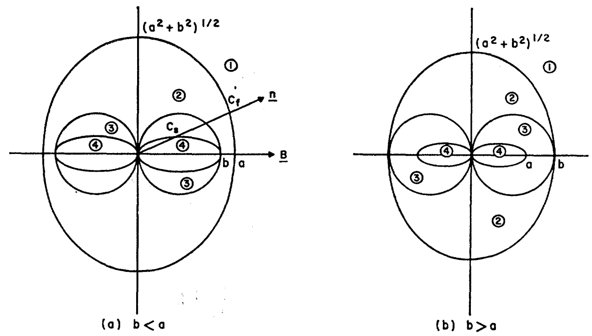

FIG. 14. Freidrichs wave speed diagram.

The stability of pure magnetohydrodynamic shock waves was recently summarized in a concise manner by Chu (78). In order to classify such shocks and summarize the known results concerning stability it is convenient to refer to the speed of propagation of a small disturbance in a plasma containing a magnetic field. [In this section we relax our restriction of a normal magnetic field and let the field have an arbitrary angle between the field and the wave normal as shown in Fig. 14 which is sometimes referred to as a Friedrichs diagram (79).] The speed in any direction θ is given by the length of the radius vector. The three waves have been named the fast wave, Alfven wave, and slow wave. With the aid of the Friedrichs diagram, solutions of the magnetohydrodynamic shock problem may be concisely and unambiguously classified. We designate the various speed regimes as (1), (2), (3), and (4) as indicated in Fig. 14. Thus, when we say that a particular shock represents a transition from region (1) to region (3), for example, we simply mean that the upstream fluid velocity relative to the shock is greater than the local fast wave speed, and the downstream fluid velocity is between the local Alfvén and slow wave speeds. The wave speed diagrams corresponding to the upstream and downstream states are always different, and it is often possible that an upstream state corresponding to Fig. 14(a) may have a downstream state corresponding to Fig. 14(b) or vice versa. In Fig. 14, a is the gas dynamic sound speed and b is the Alfven speed. When $\theta=0°$, the fast speed c_f and slow speed c_s are a and b, depending on which is greater. When $\theta=90°$, c_f is $(a^2+b_0^2)^{\frac{1}{2}}$ and c_s and b are both zero.

A necessary condition for the linearized conservation equations to possess a unique solution (i.e., be evolutionary) is that the number of outgoing waves be equal to one less than the number of equations, since the perturbation in the shock speed is also an unknown.

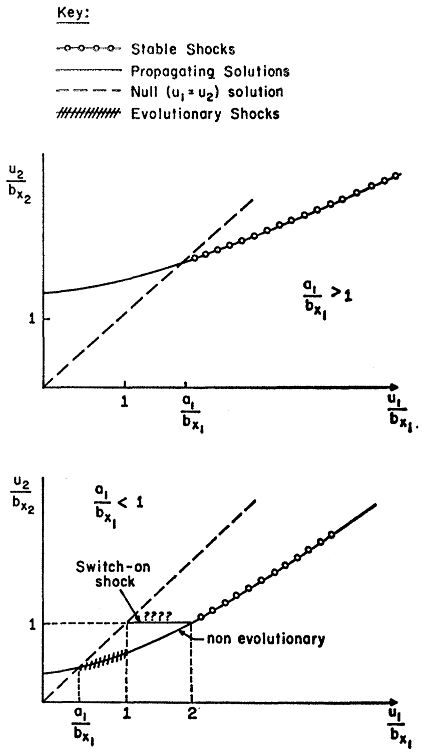

FIG. 15. Stability of normal MHD shocks.

This condition is not sufficient, and we must impose additional requirements on the independence of these equations. This necessary condition is sometimes referred to as the generalized entropy condition of Lax (80), and in the x–t plane, this condition is easily replaced as *the number of characteristics pointing away from the shock path must equal the number of jump conditions minus one.*

The only hydromagnetic shocks which are evolutionary, aside from Alfvén and contact discontinuities, *are those resulting from transitions from region* (1) *to region* (2), or from *region* (3) *to region* (4) *in Fig.* 14. *All other transitions, e.g., from* (1) *to* (3), *etc. are not evolutionary.*

The limiting cases of the switch-on and switch-off shocks [they are on the boundaries of regions (2) and (3)] are not yet known conclusively. The limit is singular, and all conclusions that the switch-on and switch-off shocks are nonevolutionary based on linear criteria are open to question. The recent work of Todd (81) suggests that if dissipation is added, the switch-on shock is stable. Recent numerical studies of the switch-on shock by Chu and Taussig (136) show their correct qualitative behavior in adjusting to plane disturbances. They conclude that under reasonable definitions, switch-on shocks are stable.

The special case of the normal magnetohydrodynamic shock wave is summarized in greater detail in Fig. 15. It has been shown that: *For* $a_1 > b_1$ (upper diagram, Fig. 15), for ($u_1 > a_1$) normal MHD shocks are stable for any polytropic gas with $\gamma < 3$ (Ref. 74). There is no switch-on solution.

For $a_1 < b_1$ (lower diagram, Fig. 15), all fast ($u_1 \gtrsim 2b_1$) MHD shocks are stable (Ref. 73) and the post-shock state is $b_{x2} < u_2 < a_2$. For switch-on shocks there is as yet no conclusive evidence for or against evolutionarity and the post-shock state is $u_2 = b_2$. MHD gas shocks in the switch-on regime ($b_1 < u_1 \lesssim 2b_1$) are nonevolutionary (Ref. 73) and the post-shock state is $u_2 < b_{x2} < a_2$. Slow ($a_1 < u_1 < b_1$) MHD shocks are evolutionary (Ref. 73), their stability is unknown, and their post-shock state is $u_2 < a_2 < b_{x2}$.

It is interesting to note that in exactly the switch-on regime ($b_1 < u_1 < 2b_1$; $u_2 < b_2 < a_2$) the MHD gas shock is unstable, (Ref. 74).

There has been no statisfactory conclusive analysis of the stability or evolutionarity of normal ionizing waves. Transverse ionizing shock waves are evolutionary (8). Even though some ionizing steady-state solutions look like those of pure gas dynamic shocks or pure MHD shocks, their stability and evolutionarity may be different because of the difference in the small signal speeds in either the pre- or post-shock gas.

XII. SHOCKED GAS TRANSPORT PROPERTIES

The transport properties of a hydrogen plasma are a subject of interest in themselves. The theory of the transport properties of an ionized gas have been extensively developed by Landshoff (82), Spitzer and Harm (83), Shkarofsky (84), and Robinson and Bernstein (85). The electromagnetic shock tube with ionizing shock waves can create interesting states of a

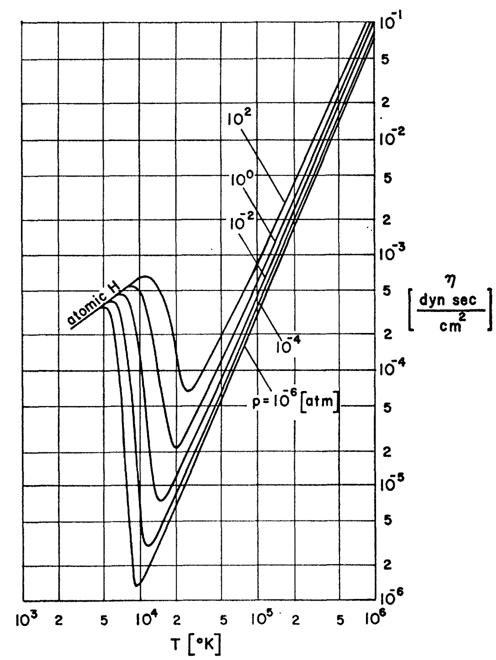

FIG. 16. Hydrogen plasma viscosity.

hydrogen plasma. The transport properties of a hydrogen plasma have been calculated over a wide range of temperature and pressures by Brezing (86). The Chapmann Enskog formalism was employed to compute the transport properties of such gas mixtures. Values of viscosity, thermal, and electrical transport coefficients as well as the thermoelectric coefficients have been calculated. Typical examples of these hydrogen plasma transport properties are shown in Figs. 16 and 17.

XIII. EXPERIMENTS

There are many laboratories throughout the world which have reported observations of experiments with strong ionizing shock waves. This research, up to about 1961, has been summarized by Kolb and Griem (70) and by Kantrowitz (67). Pioneering experimental work with strong shock waves was carried out by groups under Kantrowitz at Avco, Laporte at Michigan, Kolb at the Naval Research Laboratory, Fowler at Oklahoma, Liepmann at Cal. Tech., and Berschader at Lockheed.

In the last few years there has been a considerable expansion in experiments with strong ionizing shock waves. Although no two experimental devices are alike in detail, and the motivations are often quite different, there is sufficient interest and relevance to the theory presented earlier in this paper to mention and discuss the following experiments and observations.

Most of the experiments to date have involved shock waves whose thickness are of the order of 1 cm in hydrogen and which propagate at speeds $1\times10^4 < u_1 < 1\times10^5$ m/sec. Patrick (68) has reported waves whose speed are as high as $u_1 \approx 4\times10^5$ m/sec (presently

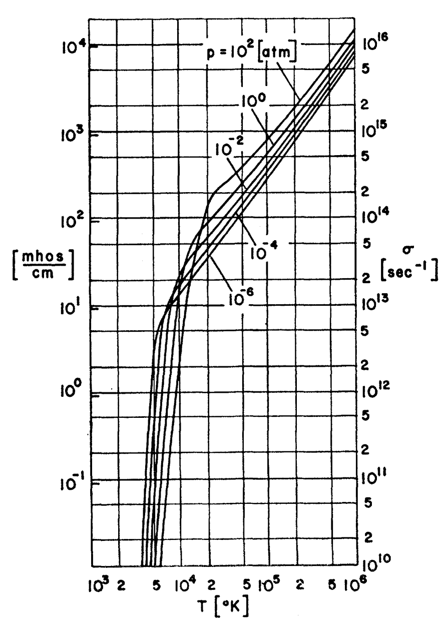

FIG. 17. Hydrogen plasma electrical conductivity.

the highest reported laboratory steady-shock speed in the literature) in which he claims to have produced a homogeneous hot plasma sample; that is, the shock and expansion fan are separated by a measurable distance. However, Kantrowitz (67) reporting on Patrick's work stated that there are still uncertainties as to the temperature behind the shock and the expansion fan has not been clearly identified.

There has been considerable interest by the Kantrowitz group, as well as others, in so-called collisionless shock waves. These waves are still the subject of intensive investigation, both theoretically and experimentally and are not considered in this review. It is however worth noting that there are as yet no laboratory-produced experiments which are clearly identified as collisionless shocks, but satellite data of the solar wind impinging on the earth's magnetosphere indicate the existence of such a shock about 14 earth radii from the earth. The author has recently learned of a claim to have observed true collisionless shocks in the laboratory; S. P. Zagorodnikov, L. I. Rudakov, G. E. Smolkin, and G. V. Sholin, Soviet Phys.—JETP **20,** 1154 (1965). There is an important difference between ionizing shock waves and collisionless shock waves. Many researchers have assumed that ionizing shocks become collisionless shocks at sufficiently high speeds. This is not so, and recently it has been pointed out that collisional interactions such as charge exchange dominate ionizing shock structure.

Patrick and Pugh (87) have recently reported on ionizing fronts and developed a semi-empirical theory to help explain them. However, their results can already be understood in terms of conventional theory provided the correct and complete system of jump equations (including the complete energy equation) are employed. The waves they observe appear to be similar to the "*N*" ionizing shock wave predicted by Taussig (9).

In the recent experiments reported on by Miller, and Miller, Levine, and Gross (11) there is reasonable agreement between the ionizing shock wave theory of Taussig (9, 10) and experimental observations. In particular they clearly identify ionizing switch-on shock waves by means of magnetic field probes. A very small (1- to 2-cm-thick) uniform plasma sample was found between the ionizing shock wave and the drive current expansion wave. In comparing data with the ionizing shock wave theory it was observed that ionizing shock waves created in their electromagnetically driven coaxial shock tube, propagate at conditions (speed, initial electric field, etc.) that just (or very nearly) correspond to the extremal points of the theory. In Fig. 18, taken from Ref. 11, the dark solid lines correspond to MHD shock wave solutions (i.e., $E_1=0$). The enclosed contours represent ionizing wave solutions, each characterized by a different initial cold gas electric field. The coordinates are the same as Fig. 15. The extremal solutions are identified by small circles on the

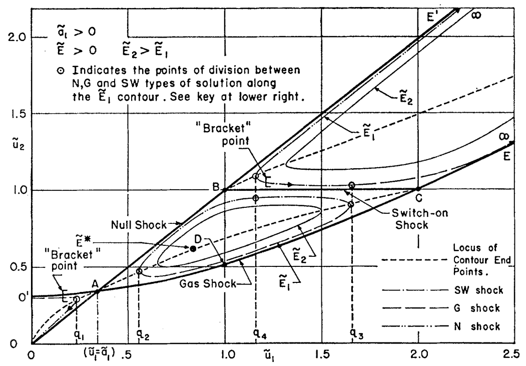

FIG. 18. Ionizing shock wave solutions.

vertical lines labeled q_1, q_2, q_3, and q_4. These external points have the property that u_2= slow wave speed in the post shock gas. These points are therefore quite similar to the Chapman–Jouguet state of gaseous detonation wave theory.

An interesting and physically appealing picture is proposed, based upon these observations. Consider a metallic wall coaxial electromagnetic shock tube containing a cold-nonconducting gas. When a high voltage is placed across the shock tube a series of electromagnetic waves propagate back and forth along this waveguide. These waves die down in a few nanoseconds to produce a radial electric field in the cold gas just equal to the impressed field. Then the gas in the tube begins to electrically break down, current starts to flow across the tube, electric charges along the tube walls redistribute themselves with some flowing through the gas, and the newly formed ionizing shock wave starts to accelerate into the cold gas which contains a continually changing (decreasing) initial electric field. The post shock plasma speed (u_2) increases until it attains the slow, small disturbance wave speed. The flow behind the ionizing wave is then choked, analogous to a Chapman–Jouguet wave. The ionizing wave then continues to propagate at a steady speed with conditions representative of the extremal points of ionizing shock wave theory. These extremal points also have the property that the expansion wave front moves at the shock wave speed, i.e., there is no uniform post shock plasma sample. The locus of extremal solutions lies along the line $xe/x_s = 1$ in Fig. 13. This observation, that electromagnetically driven ionizing shock waves move at conditions equal to (or nearly equal to) the extremal solution, helps to explain the previous frustrating inability of numerous investigators to find the sought after uniform plasma sample behind the ionizing shock wave. The initial value, transient description just given also yields which of the numerous theoretical solutions should be found at a given steady ionizing wave speed—namely that of the extremal solution at that speed.

Although T tubes do not produce a steady velocity shock wave, but rather a decaying blast-like shock wave, they have contributed notably advances in experimental shock tube work. Particularly noteworthy is the pioneering work using the T tube for spectroscopic work of Kolb (88), Kolb and Griem (70), McClean (89), Fowler *et al.* (90, 91), and Turner (92). Most of these experiments use the shock heated gas to generate radiation which in turn is used to measure atomic properties such as f numbers and collisional line broadening coefficients. There is considerable concern in such experiments as to the actual attainment of local thermodynamic equilibrium. For a detailed discussion of the requirements for this state, one can refer to the recent book by Griem (93). Since the shock wave speed in a T tube varies in time, the structure of the gas behind the shock wave is nonuniform in temperature. T tubes can create a hydrogen plasma whose temperature is up to about 20 000°K. Others who have reported on T tube experiments are Cloupeau (94), and Jeanmaire (95), both of whom developed interesting optical studies of the wave progression, but their results were mainly qualitative. Fowler (96) explained why Cloupeau did not observe the expected separation of driver gas from the shock front. Conical electrically driven shock tubes have been used, as another means to produce a strong but decaying shock wave by Bershader (97) and Makarov and Nartov (98).

There have been many experiments with cylindrical shock waves, particularly those associated with pinch dynamic studies in thermonuclear research. Most of these studies simplify the problem to that of the snow plow model and concentrate their attention upon the stability of the pinched configuration. Of particular interest, however, to this study of ionizing shock waves is the work of Vlases (99, 100). With an inverse pinch he has demonstrated some of the qualitative differences between an ionizing wave, a gas dynamic shock and an MHD shock. Unfortunately, the scale of his experiments were too small for quantitative work.

Plasma guns, as used for plasma production in thermonuclear research and space propulsion have some features of strong shock waves. The works of Mawardi (101), Keck (102), and Wilcox *et al.* (103) are particularly relevant and are contained in the proceedings of an international symposium on plasma guns, published as a supplement to the *Physics of Fluids*, Vol. 7, No. 11 (1964). Plasma guns offer little hope, however, in producing a uniform plasma of well-known structure and physical state, or in producing very high temperatures.

A very interesting and unique study of an ionizing shock wave was carried out in a pressure driven shock tube by Haught (104) using cesium. He concentrated on the thermal ionization rate process in cesium and showed that it took place in a two-step process.

Coaxial geometry, electromagnetically driven shock tubes with steady drive currents are reported upon by several laboratories. Besides the early work of Patrick (68) and later Patrick and Pugh (87) at Avco, such shock tube experiments have been reported upon by Gross, Miller, and Levine at Columbia University (11), Wilcox *et al.* at the University of California, Berkeley (105), Watson-Munro *et al.* at the University of Sydney, Australia (106–108), Heiser at MIT (109), Block and Naraghi at Case Institute (110, 111), Yasuhara *et al.* at Tokyo University (112), and Koopman at the University of Michigan (113).

Keck (114) and Fishman and Petschek (115) reported on the radius ratio effect in such coaxial tubes. If the outer to inner radius gets too large, the nonuniform magnetic field behind the drive current causes a tilt in the current distribution and makes the experiment hard to interpret.

Although few investigators report in sufficient detail the electric drive currents and the wave speeds they generate, it appears that the wave speeds produced are at times lower than that which the simple shock tube model predicts. The experiments of Brennan *et al.* (106) have verified the analytical approximate wave speed predictions of Kunkel and Gross (5).

Heiser (109) has some evidence that he had produced a switch-on wave but the data contains great scatter and is not conclusive. Most continuum radiation measurements which claim to be quantitative must be viewed with great skepticism unless the investigator has exercised great care with gas cleanliness (lack of impurities) in the shock heated gas. This is a very difficult experimental problem when large electrical currents are present. Since bremstrahlung varies with the square of atomic weight, a very small percentage of impurities, such as O, C, etc. will greatly exceed the continuum radiation from hydrogen.

The hypothesis of Alfvén (116) concerning a critical velocity corresponding to the ionization energy of the atom (about 2×10^4 m/sec for hydrogen) does not seem to be upheld by the detailed calculations of Taussig (10). There is no steep barrier for wave speed vs drive current as can be seen in Fig. 12. The effect of ionization does change the slope of the curve in Fig. 12 and the resultant post-shock temperature is reduced as shown in Fig. 1. However, increasing drive current results in increasing wave speed. The fact that many investigators have reported ionizing shock wave speeds of about 2×10^4 m/sec may be related to the initial electric field present in the cold gas and the fact that the lower speed of such bounded ionizing shock wave solutions is about 2×10^4 m/sec. The work of Pearson and Kunkel (117) on ionization rates in crossed electric and magnetic fields makes plausible the frequently observed shock speeds of about 2×10^4 m/sec. This speed seems to depend principally upon the ionization rate phenomena in the wave itself which is in turn reflected in the initial upstream electric field.

In nearly all experiments with strong shock waves there are reports and observations of free electrons in the cold pre-shocked gas. They were reported in 1960 by Weymann (118) in experiments with a gas driven shock tube at Mach numbers as low as about 10. Gloersen (119) also observed such precursor electrons at about the same time. They were also observed by Jones (120) in 1962 and Wetzel (121) developed a theory based upon electron diffusion from the shock heated gas. Wetzel in 1963 developed another theory based upon photon absorption to explain precursor electrons. Gerardo, *et al.* (122) reported observing precursor electrons by using microwave diagnostics, and they postulated on the formation of these electrons from x rays from the anode in the discharge. Groening (123) also reported precursor studies and Pipkin (124) partially explained some precursor observations. Barach (125) and Hill (126) give further observations of precursors using different measuring techniques, and they discuss some of the problems in such measurements. Ferrari and Clarke (127) have developed a diffusion theory for precursor electrons.

A brief recent review of the theories of fast luminous fronts which preceed shock waves in electromagnetically driven shock tubes has been made by Nelson (128). The present literature has come alive with qualitative observations of precursor electrons. The details differ from experiment to experiment and the physical causes are still uncertain. The hot electrons predicted by Jaffrin and Probstein (27) which propagate with the same speed as the shock wave and the photon absorption studies like those reported upon by Whitney (48) are relevant. There is little doubt that precursor electrons are often present in strong shock experiments, but the detailed causes and their true importance remain to be explained and explored.

Some astrophysical observations may be classified as experiments; i.e., real plasma phenomena but not under the control of the observer. Tidman (129) analyzed the shock structure from solar noise of type II bursts. Will, Smerd, and Weiss (130) reviewed the known facts about solar bursts.

The reproducibility and reliability of all reported experiments on strong ionizing waves reported to date leaves much to be desired. The state of development of the electromagnetically driven shock tube is still young, changing and improving. It promises to open up the experimental field of thermal physics in a wide energy range.

ACKNOWLEDGMENTS

It is a pleasure to acknowledge the important contributions to this paper made by R. Taussig and P. Koch. I am grateful to Dr. C. K. Chu for his many contributions to this paper and his constructive review. The members of the Columbia Plasma Laboratory also helped greatly by their many fruitful discussions. This research has been carried out under sponsorship of the U. S. Air Force Office of Scientific Research under contract AFOSR 49(638)-1254.

REFERENCES

[1] A. G. Kulikovskii and G. A. Lyubimov, Rev. Mod. Phys. **32**, 977 (1960).
[2] G. A. Lyubimov, Doklady Akad. Nauk. SSSR **126**, 291 (1959).

[3] A. G. Kulikovskii and G. A. Lyubimov, Doklady Acad. Nauk SSSR **129,** 52 (1959).
[4] G. A. Lyubimov and A. G. Kulikovskii, Doklady Acad. Nauk SSSR **129,** 525 (1959).
[5] W. B. Kunkel and R. A. Gross, "Hydromagnetic Ionizing Waves," in *Plasma Hydrodynamics* (Stanford University Press, Stanford, California, 1962), pp. 58–82.
[6] J. B. Helliwell and D. C. Pack, Phys. Fluids **5,** 738 (1962).
[7] J. B. Helliwell, Phys. Fluids **6,** 1516 (1963).
[8] C. K. Chu, Phys. Fluids **7,** 1349 (1964).
[9] R. Taussig, "Normal Ionizing Shock Waves," Phys. Fluids (to be published).
[10] R. Taussig, "Normal Ionizing Shock Waves—The Effects of Equilibrium Dissociation and Ionization," Columbia Univ. Plasma Lab. Rept. 14 (August 1964).
[11] B. Miller, "Ionizing Shock Studies in an Electromagnetically Driven Shock Tube," Columbia University Plasma Lab. Rept. 19, June 1965 (thesis); also see B. Miller, L. Levine, and R. A. Gross, "Ionizing Shock Studies in an Electromagnetically Driven Shock Tube," in *Proceedings of the Fifth Shock Tube Symposium,* U.S. Naval Res. Lab., 28–30 April 1965 (to be published).
[12] R. Becker, Z. Physik **8,** 321 (1921–1922).
[13] D. Gilbarg, Am. J. Math. **73,** 256 (1951).
[14] D. Gilbarg and D. Paolucci, J. Ratl. Mech. Anal. **2,** 617 (1953).
[15] C. S. Chang Wang, Appl. Phys. Lab. Rept. No. APL/JHU CM 503 (1948).
[16] H. M. Mott-Smith, Phys. Rev. **82,** 885 (1951).
[17] K. Zoller, Z. Physik **130,** 1 (1951).
[18] H. Grad, Commun. Pure Appl. Math. **5,** 257 (1952).
[19] W. Marshall, Proc. Roy Soc. (London) **A233,** 367 (1955).
[20] J. Bergers, in *Magnetohydrodynamics,* edited by R. K. M. Landshoff (Stanford University Press, Stanford, California, 1957).
[21] G. S. S. Ludford, J. Fluid Mech. **5,** 67 (1959).
[22] P. Germain, Rev. Mod. Phys. **32,** 951 (1960).
[23] B. A. Tverskoi, Soviet Phys.—JETP **19,** 1118 (1964).
[24] R. V. Deutsch, Soviet Phys.—JETP **16,** 475 (1963).
[25] J. E. Anderson, *Magnetohydrodynamic Shock Waves* (Technology Press, Cambridge, Massachusetts, 1963).
[26] V. Nemytskii and V. Stepanov, *Qualitative Theory of Differential Equations* (Princeton University Press, Princeton, New Jersey, 1960).
[27] M. Y. Jaffrin and R. F. Probstein, Phys. Fluids **7,** 1658 (1964).
[28] V. S. Imshennik, Soviet Phys.—JETP **15,** 167 (1962).
[29] F. S. Sherman and L. Talbot, *Rarified Gas Dynamics,* edited by F. M. Devienne (Pergamon Press, Inc., New York, 1960), pp. 161–191.
[30] J. D. Jukes, J. Fluid Mech. **3,** 275 (1957).
[31] V. D. Shafranov, Soviet Phys.—JETP **5,** 1183 (1957).
[32] O. W. Greenberg, H. K. Sen, and Y. M. Treve, Phys. Fluids **3,** 379 (1960).
[33] O. W. Greenberg and Y. M. Treve, Phys. Fluids **3,** 769 (1960).
[34] M. S. Grewal and L. Talbot, J. Fluid Mech. **16,** 573 (1963).
[35] M. Y. Jaffrin, MIT Fluid Mechs. Lab. Publ. No. 64–9 (October 1964).
[36] R. M. May and J. Tendys (private communication).
[37] R. G. Sacks, Phys. Rev. **69,** 514–522 (1946).
[38] A. W. Guess and A. K. Sen, *Conference on Extremely High Temperature* (John Wiley & Sons, Inc., New York, 1958).
[39] V. A. Prokof'ev, Uch. Zap. Mosk. Gos. Univ., Mech. **172,** 79 (1952).
[40] J. F. Clarke, Phys. Fluids **5,** 1347 (1962).
[41] Ia. B. Zel'dovich, Soviet Phys.—JETP **5,** 919 (1957).
[42] M. A. Heaslet and B. S. Baldwin, Phys. Fluids **6,** 781 (1963).
[43] M. Mitchner and M. Vinokur, Phys. Fluids **6,** 1682 (1963).
[44] R. E. Marshak, Phys. Fluids **1,** 24 (1958).
[45] S. C. Trangott, *Proceedings of the* 1963 *Heat Transfer and Fluid Mechanics,* edited by A. Roshko *et al.* (Stanford University Press, Stanford, California, 1963).
[46] S. M. Scala and D. H. Sampson, *Heat Transfer in Hypersonic Flow with Radiation and Chemical Reaction,* edited by D. Olfe (Pergamon Press, Inc., New York, 1963).
[47] J. Pomerantz, J. Quant. Spect. Rad. Trans. **1,** 185 (1961).
[48] C. A. Whitney and A. J. Skalafuris, Astrophys. J. **138,** 200 (1963).
[49] F. A. Goldsworthy, Phil. Trans. Roy. Soc. London **A253,** 277, 1028 (1961).
[50] W. I. Axford, Phil. Trans. Roy. Soc. London **A253,** 301, 1029 (1961).
[51] W. I. Axford, Astrophy J. **140,** 112 (1964).
[52] P. Koch, "On Radiative Shock Structure." Columbia Univ. Plasma Lab. Rept. 9, March 1964, Ph.D. thesis.
[53] D. H. Menzel and C. L. Pekeris, Monthly Notices Roy. Astron. Soc. **96,** 1 (November 1935).
[54] S. Chandrasekhar, *Stellar Structure* (Dover Publications, Inc., New York, 1957).
[55] C. Eckhard, Phys. Rev. **58,** 919 (1940).
[56] A. H. Taub, Phys. Rev. **74,** 328 (1948).
[57] L. D. Landau and E. M. Lifshitz, *Fluid Mechanics* (Pergamon Press, Inc., New York, 1959), Chap. XV.
[58] J. L. Synge, *The Relativistic Gas* (North-Holland Publishing Company, Amsterdam, and Interscience Publishers, Inc., New York, 1957).
[59] F. de Hoffman and E. Teller, Phys. Rev. **80,** 692 (1950).
[60] L. M. Kovrezhnykh, Soviet Phys.—JETP **12,** 725 (1961).
[61] A. Masani, Nuovo Cimento **24,** 1066 (1962); and **29,** 224 (1963).
[62] M. Schwartzschild, Trans. Intern. Astron. Union **8,** 811 (1952).
[63] A. Kaplan and G. Klemishin, Soviet Astron.—AJ **36,** 404 (1959).
[64] L. D. Landau and E. M. Lifshitz, *Statistical Physics* (Addison-Wesley Publishing Company, Reading, Massachusetts, 1958), Vol. 5, Theoretical Physics, Chapter XI.
[65] A. Simon, *An Introduction to Thermonuclear Research* (Pergamon Press, Inc., New York, 1962), 2nd ed.
[66] A. A. Barmin, Soviet Phys.—Doklady **6,** 374 (1961).
[67] A. Kantrowitz, "Shock Tubes for High Temperature Gas Kinetics," 15th Anniversary Solvay Conference, Brussels, Belgium, 1962; also AVCO AERL RR 141 October 1962.
[68] R. M. Patrick, Phys. Fluids **2,** 589 (1959).
[69] N. H. Kemp and H. E. Petschek, Phys. Fluids **2,** 599 (1959).
[70] A. C. Kolb and H. R. Griem, *Atomic and Molecular Processes,* edited by D. R. Bates (Academic Press Inc., New York, 1962), Chap. V.
[71] J. K.Wright and M. C. Black, J. Fluid Mech. **6,** 289 (1959).
[72] J. Hart, J. Appl. Phys. **35,** 3425 (1964).
[73] A. Jeffrey and T. Taniuti, *Nonlinear Wave Propagation with Applications to Physics and Magnetohydrodynamics* (Academic Press Inc., New York, 1964).
[74] C. S. Gardner and M. D. Kruskal, Phys. Fluids **7,** 700 (1964).
[75] A. I. Akhiezer, G. J. Lyubarskii, and R. V. Polovin, Soviet Phys.—JETP **8,** 507 (1959).
[76] S. I. Syrovatskii, Soviet Phys.—JETP **8,** 1024 (1959).
[77] R. V. Polovin, Soviet Phys.—Uspekhi **3,** 677 (1961).
[78] C. K. Chu, "Hydromagnetic Shock Waves and Ionizing Shock Waves," in *Proceedings of* 14*th National Applied Mechanics Congress of Japan* (to be published).
[79] K. O. Friedrichs, "Nonlinear Wave Motion in Magnetohydrodynamics," Los Alamos Rept. LAMS 2105 (1954), revised and reissued as N. Y. U. Rept. NYO 6486 VIII (1958).
[80] P. D. Lax, Commun. Pure. Appl. Math. **10,** 537 (1957).
[81] L. Todd, J. Fluid Mech. **18,** 321 (1964).
[82] R. Landshoff, Phys. Rev. **82,** 442 (1951).
[83] L. Spitzer, Jr., and R. Harm, Phys. Rev. **89,** 977 (1953).
[84] I. P. Shkarofsky, Can. J. Phys. **39,** 1619 (1961).
[85] B. B. Robinson and I. B. Bernstein, Ann. Phys. (N. Y.) **18,** 110 (1962).
[86] D. Brezing, "Transport Properties of Hydrogen", Columbia Univ. Plasma Lab. Rept. 13 (September 1964); also, Am. Inst. Aeron. Astronaut. **3,** 1422 (1965).
[87] R. M. Patrick and E. R. Pugh, Phys. Fluids **8,** 636 (1965).
[88] A. C. Kolb *et al.* in *Proceedings of the Fourth International Conference on Ionization Phenomena in Gases, Upsala, 1959,* edited by N. R. Nilsson (North-Holland Publishing Company, Amsterdam, 1960), Vol. II, p. 1021; see also: *Plasma Dynamics,* edited by F. H. Clausner (Addison-Wesley Publishing Company, Reading, Massachusetts, 1960), p. 206; *Symposium on Optical Spectro Measurements of High Temperature* (University of Chicago Press, Chicago, 1961); *Magnetohydrodynamics,* edited by R. K. M. Landshoff (Stanford University Press, Stanford, California, 1957).
[89] E. A. McClean, Phys. Fluids **3,** 843 (1960); Phys. Fluids **4,** 8, 1055 (1961); Third Symp. on Temp.; Its Measurement and Control in Science and Industry, 1961, Columbus, Ohio.
[90] R. G. Fowler, W. R. Atkinson, W. D. Compton, and R. J. Lee, Phys. Rev. **88,** 137 (1952).
[91] R. G. Fowler and B. D. Fried, Phys. Fluids **4,** 767 (1961).
[92] E. B. Turner and R. G. Fowler, Phys. Fluids **4,** 544 (1961).
[93] H. R. Griem, *Plasma Spectroscopy* (McGraw-Hill Book Company, Inc., New York, 1964).

[94] M. Cloupeau, Phys. Fluids **6**, 5, 679 (1963); also Compt. Rend. **254**, 213 (1962); **253**, 1160 (1961); and **251**, 918 (1960).
[95] P. Jeanmaire, Phys. Fluids **6**, 1028 (1963).
[96] R. G. Fowler, Phys. Fluids **6**, 548 (1963).
[97] D. Bershader, Rev. Mod. Phys. **32**, 780 (1960).
[98] Yu. V. Makarov and S. V. Nartov, Soviet Phys.—Tech. Phys. **8**, 541 (1963).
[99] G. C. Vlases, J. Fluid Mech. **16**, 82 (1963).
[100] G. C. Vlases, Phys. Fluids **7**, 1358 (1964).
[101] O. K. Mawardi, Phys. Fluids **7**, Part 2, S9 (November 1964).
[102] J. Keck, Phys. Fluids **7**, Part 2, S16 (November 1964).
[103] J. M. Wilcox, E. Pugh, A. Dattner, and J. Eninger, Phys. Fluids **7**, Part 2, S51 (November 1964).
[104] A. F. Haught, Phys. Fluids **5**, 1337 (1962).
[105] J. M. Wilcox, F. I. Boley, and A. W. DeSilva, Phys. Fluids **3**, 15 (1960).
[106] M. H. Brennan, I. G. Brown, P. P. Millar, and C. N. Watson-Munro, J. Nucl. Energy, Part C, Plasma Phys. **5**, 229 (1963).
[107] M. H. Brennan, J. A. Lehane, D. D. Millar, and C. N. Watson-Munro, Australian J. Phys. **16**, 340 (1963).
[108] L. Sharp and C. N. Watson-Munro, Phys. Rev. Letters **11**, 39 (1964).
[109] W. H. Heiser, Phys. Fluids **7**, 143 (1964); also, "Axial Field Effects in a Magnetically Driven Shock Tube," MIT, R. L. E. Tech. Rept. 408 (29 March 1963).
[110] R. B. Block, "The Onset of an Electromagnetic Shock Wave," Case Inst. Tech. Rept. No. A-23 (July 1963).
[111] M. Naraghi, "A Study of Current Sheets in a Coaxial Plasma Gun," Case Inst. Tech. Rept. No. A-22 (June 1963).
[112] M. Yasuhara, S. Tsuboi, and K. Ban, Tokyo, Univ. Aeron. Res. Lab. Rept. **3**, Special issue (September 1963).
[113] D. W. Koopman, Phys. Fluids **7**, 1651 (1964).
[114] J. C. Keck, Phys. Fluids. **5**, 630 (1962).
[115] F. J. Fishman and H. Petschek, Phys. Fluids **5**, 632 (1962).
[116] H. Alfven, Rev. Mod. Phys. **32**, 710 (1960).
[117] G. A. Pearson and W. B. Kunkel, *Proceedings of the International Conference on Ionizing Phenomena in Gases, Paris, 1963*, edited by P. Hubert and E. Cremieu-Alcan (Minister of State in Charge Scientific Research pertaining to Atomic and Spacial Matter, Paris, 1963), Vol. I, p. 259; See also Phys. Rev. **130**, 864 (1963); Also UCRL Rept. 10366.
[118] H. D. Weymann, Phys. Fluids **3**, 545 (1960).
[119] P. Gloersen, Phys. Fluids **3**, 857 (1960).
[120] D. L. Jones, Phys. Fluids **5**, 824 (1962).
[121] L. Wetzel, Phys. Fluids **5**, 824 (1962); **6**, 750 (1963); **6**, 1660 (1963).
[122] J. B. Gerardo, C. D. Henricks, and L. Goldstein, Phys. Fluids **6**, 1222 (1963).
[123] H. Groening, Phys. Fluids **6**, 142 (1963).
[124] A. C. Pipkin, Phys. Fluids **6**, 1382 (1963).
[125] J. P. Barach and J. A. Sivinski, Phys. Fluids **7**, 1075 (1964).
[126] R. J. Hill, Phys. Fluids **7**, 1865 (1964).
[127] C. Ferrari and J. H. Clarke, Brown Univ. Rept. Cm 1020 (1963).
[128] R. A. Nelson, Phys. Fluids **8**, 23 (1965).
[129] D. A. Tidman, Phys. Fluids **5**, 1104 (1962).
[130] J. P. Wild, S. F. Smerd, and A. A. Weiss, Ann. Rev. Astron. Astrophys. **1**, 291 (1963).
[131] S. A. Colgate, W. H. Grasberger, and R. H. White, J. Phys. Soc. Japan **17**, Supplement A, 111 (1962), Part III.
[132] M. H. Johnson and S. A. Colgate, Phys. Rev. Letters **5**, (1960).
[133] I. M. Cohen and J. H. Clarke, "The Influence of Viscosity on Shock Waves Structured by Radiation," Div. Engr. Brown Univ. Rept. Nonr. (562)35/5, October 1964.
[134] Z. O. Bleviss, *The Structure of a Steady Magnetohydrodynamic Switch-on Shock Wave* (Stanford University Press, Stanford, California, 1959); also, Douglas Rept. No. SM 23720, Santa Monica Div. (October 1959).
[135] H. E. Petcheck and S. Byron, Ann. Phys. (N. Y.) **1**, 270 (1957).
[136] C. K. Chu and R. Taussig (private communication); see also Proc. 1965 Appl. Math. Symp., Am. Math. Soc. (to be published).

REVIEWS OF MODERN PHYSICS VOLUME 37, NUMBER 4 OCTOBER 1965

Stimulation of Zinc Sulfide and Similar Inorganic Phosphors

D. E. MASON*

Electrical Engineering Department, University of Manchester, Manchester, England

Further support is provided for a model of the stimulation process in inorganic phosphors recently proposed by Luchner, Kallmann, Kramer, and Wachter. A reasonable identification of the center responsible for the absorption of stimulating radiation (the main feature of this model) is made for zinc sulfide phosphors containing copper, but it is shown that no identification can be made as yet of the absorbing centers responsible for most of the peaks of stimulation spectra so far observed. Many of the apparently incompatible published observations can be reconciled with the aid of previously unpublished work.

I. INTRODUCTION

In a recent paper by Luchner, Kallmann, Kramer, and Wachter,[1] a model for the stimulation process (in which the luminescence of a previously excited phosphor is temporarily enhanced by long-wavelength radiation incapable of exciting it) is proposed, which may, with profit, be enlarged upon. In this way, the conflicting views of various authors may, to some extent, be resolved, using their own data as well as previously unpublished work of the author.[2]

The model of Luchner *et al.* (which we will call the LKKW model) is outlined below:

1. Trapped electrons exist mainly in the neighborhood of ionized activators and are coupled to them.
2. An infrared quantum is absorbed by the complex

* A member of the staff of Ferranti Ltd., Manchester, England.
[1] K. Luchner, H. Kallmann, B. Kramer, and P. Wachter, Phys. Rev. **129**, 593 (1963).

[2] D. E. Mason, Ph.D. thesis, University of Birmingham, England, 1950 (unpublished).